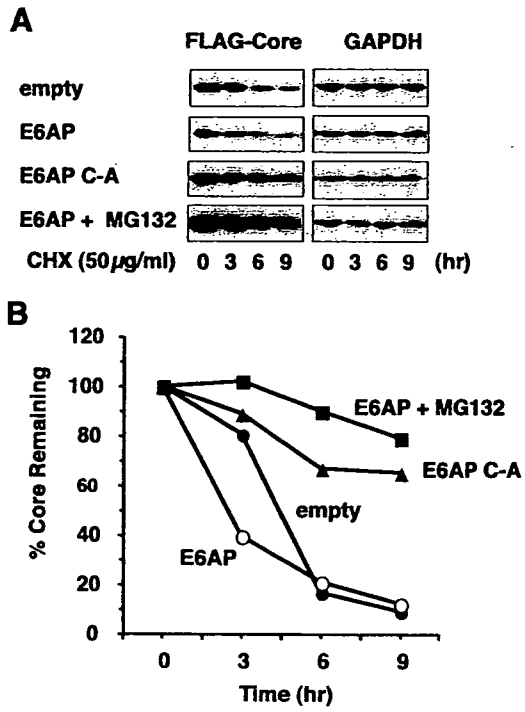

FIG. 5. Kinetic analysis of E6AP-dependent degradation of HCV core protein. (A) 293T cells (1×10^6 cells/10-cm dish) were transfected with 1 μg of pCAG-FLAG core (1–152) plus 4 μg of empty vector, pCMV-HA-E6AP, or pCMV-HA-E6AP C-A. The cells were treated with 50 μg/ml CHX at 44 h after transfection. Cell extracts were collected at 0, 3, 6, and 9 h after treatment with CHX, followed by immunoblotting. (B) Specific signals were quantitated by densitometry, and the percent remaining core at each time was compared with that at the starting point. The level of GAPDH served as a loading control. Open circles, E6AP; closed circles, empty plasmid; closed triangles, E6AP C-A; closed squares, E6AP with MG132 treatment. Data are representative of three independent experimental determinations.

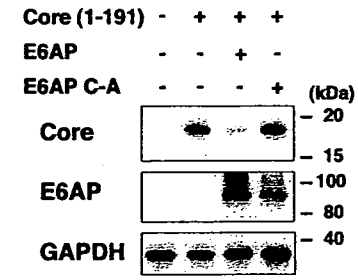

FIG. 6. E6AP promotes degradation of full-length HCV core protein in Huh-7 cells. Huh-7 cells (2×10^5 cells/six-well plate) were transfected with 0.5 μg of pCAG-core (1–191) together with 2 μg of pCMV-HA-E6AP or pCMV-HA-E6AP C-A. At 48 h posttransfection, cells were harvested and analyzed by immunoblotting with anticore MAb (top panel), anti-E6AP PAb (middle panel), or anti-GAPDH MAb (bottom panel).

levels of the core protein in hepatic cells as well as in 293T cells. Exogenous expression of E6AP resulted in reduction of the core protein in human hepatoblastoma HepG2 cells (Fig. 4D). Treatment of the cells with the proteasome inhibitor MG132 increased the core protein level, suggesting that the core protein was degraded through the ubiquitin-proteasome pathway. These results indicate that E6AP enhances proteasomal degradation of the HCV core protein in both hepatic cells and nonhepatic cells.

Kinetic analysis of E6AP-dependent degradation of HCV core protein. To determine whether the E6AP-induced reduction of the core protein is due to an increase in the rate of core degradation, we performed kinetic analysis using the protein synthesis inhibitor CHX. HCV core protein together with wild-type E6AP or inactive mutant E6AP C-A was expressed in 293T cells. At 44 h after transfection, cells were treated with either 50 μg/ml CHX alone or 50 μg/ml CHX plus 25 μM MG132 to inhibit proteasome function. Cells were collected at 0, 3, 6, and 9 h following treatment and analyzed by immunoblotting (Fig. 5A). Overexpression of E6AP resulted in rapid degradation of the core protein, whereas inactive mutant E6AP C-A increased the half-life of the core protein (Fig. 5B), suggesting that the inactive E6AP inhibited degradation of the core protein in a dominant-negative manner, which is in agreement with previous studies (19, 55). Treatment of the cells with MG132 inhibited the degradation of the core protein (Fig. 5B). Reverse transcription-PCR to determine mRNA levels of the HCV core gene and GAPDH gene found that neither wild-type E6AP nor inactive E6AP changed mRNA levels of the HCV core gene and GAPDH gene (data not shown). These results indicate that E6AP enhances proteasomal degradation of the core protein.

E6AP promotes degradation of the full-length core protein in Huh-7 cells. To determine whether the full-length HCV core protein expressed in hepatic cells is degraded through an E6AP-dependent pathway, human hepatoma Huh-7 cells were transfected with pCAG HCV core (1–191) along with either E6AP or E6AP C-A. To rule out the effects of N-terminal FLAG tag on the core degradation, HCV core protein was expressed as untagged protein. Expression of wild-type E6AP resulted in reduction of the core protein (Fig. 6). On the other hand, HCV core protein was not decreased after transfection of inactive E6AP, indicating that the full-length core protein expressed in Huh-7 cells is also degraded through an E6AP-dependent pathway.

E6AP mediates ubiquitylation of HCV core protein in vivo. To determine whether E6AP can induce ubiquitylation of HCV core protein in cells, we performed in vivo ubiquitylation assays. 293T cells were cotransfected with FLAG-core (1–191) and either E6AP or empty plasmid, together with a plasmid encoding HA-tagged ubiquitin to facilitate detection of ubiquitylated core protein. Cell lysates were immunoprecipitated with anti-FLAG MAb and immunoblotted with anti-HA PAb to detect ubiquitylated core protein (Fig. 7A). Only a little ubiquitin signal was observed on the core protein in the absence of cotransfected E6AP (Fig. 7A, lane 3). In contrast, coexpression of E6AP led to readily detectable ubiquitylated forms of the core protein as a ladder and a smear of higher-molecular-weight bands (Fig. 7A, compare lane 3 with lane 4). Immunoblot analysis with anticore PAb confirmed that FLAG-core proteins were immunoprecipitated (Fig. 7B, lanes 2 to 4, short exposure) and that higher-molecular-weight bands con-

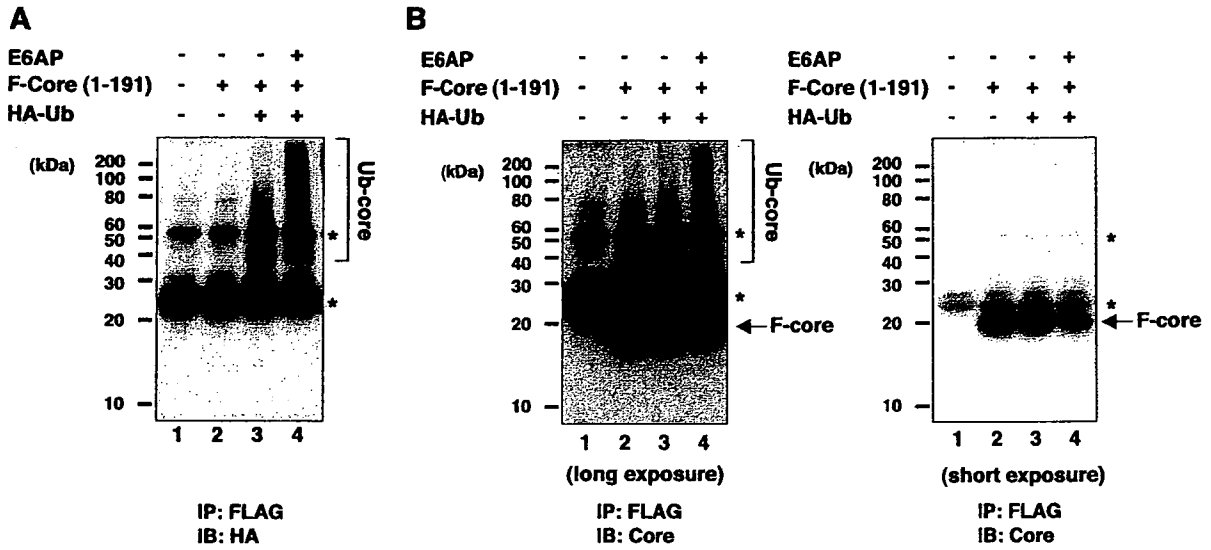

FIG. 7. E6AP-dependent ubiquitylation of HCV core protein in vivo. 293T cells (1×10^6 cells/10-cm dish) were transfected with 1 μg of pCAG FLAG-core (1–191) together with 2 μg of plasmid encoding E6AP as indicated. Each transfection also included 2 μg of plasmid encoding HA-ubiquitin. The cell lysates were immunoprecipitated with FLAG beads and analyzed by immunoblotting with anti-HA PAb (A) or anticore PAb (B). A shorter exposure of the core blot shows immunoprecipitated FLAG-core protein (B, right panel). A longer exposure of the core blot shows the presence of a ubiquitin smear (B, left panel). Asterisks indicate cross-reacting immunoglobulin light chain or heavy chain. Arrows indicate FLAG-core. IB, immunoblot; IP, immunoprecipitation.

jugated with HA-ubiquitin were indeed ubiquitylated forms of the core protein (Fig. 7B, lanes 3 and 4, long exposure).

E6AP mediates ubiquitylation of HCV core protein in vitro. To rule out the possibility that E6AP contributes to core protein degradation by inducing degradation of inhibitors of core turnover, we determined whether E6AP functions directly as a ubiquitin ligase by testing the ability of purified MEF-E6AP to mediate in vitro ubiquitylation of the purified recombinant HCV core protein. HCV core protein was expressed as a fusion protein containing N-terminal GST tag and C-terminal His tag and purified as described in Materials and Methods. GST-C173HT (aa 1–173) and GST-C152HT (aa 1–152) (see Materials and Methods) were used to determine whether the mature core protein and the C-terminally truncated core protein are targeted for ubiquitylation in vitro. The validity of this assay was established by demonstrating that E6AP but not E6AP C-A induced ATP-dependent ubiquitylation of GST-core protein. When in vitro ubiquitylation reactions were carried out either in the absence of MEF-E6AP or in the presence of MEF-E6AP C-A, no ubiquitylation signal was detected (Fig. 8A, lanes 4 and 5). However, inclusion of purified MEF-E6AP in the reaction mixture resulted in marked ubiquitylation of GST-C173HT (Fig. 8A, lane 6), while no ubiquitylation was observed in the absence of ATP (Fig. 8A, lane 7). No signal was detected when GST-HT was used as a substrate (Fig. 8A, lane 8). The higher-molecular-weight species of GST-core proteins were reactive with both anti-ubiquitin MAb (Fig. 8B, right panel, lanes 2 and 4) and anti-GST MAb (Fig. 8B, left panel, lanes 2 and 4). Both GST-C152HT and GST-C173HT were polyubiquitylated by E6AP in vitro (Fig. 8B), indicating that both the C-terminally truncated core and the mature core are polyubiquitylated by E6AP in vitro. These results revealed that E6AP directly mediated ubiquitylation of HCV core proteins in an ATP-dependent manner.

Exogenous expression of E6AP reduces intracellular HCV core protein levels and supernatant infectivity titers in HCV-infected Huh-7 cells. We used a recently developed system for the production of infectious HCV particles using the HCV JFH1 strain (28, 56, 61) to examine whether E6AP can promote degradation of HCV core protein expressed from infectious HCV. E6AP-dependent core degradation was assessed in Huh-7 cells inoculated with the culture supernatant containing HCV JFH1. Levels of HCV core protein were detectable at day 3 postinfection and increased with time. Immunofluorescence staining for the core protein indicated that the percentage of HCV core-positive cells in the Huh-7 cells was almost 100 at day 7 postinfection. Transfection efficiency was 50 to 60% as measured with GFP-expressing plasmid. At day 7 postinfection, exogenous expression of E6AP reduced the intracellular core protein level by about 60% compared to the empty plasmid-transfected control cells (Fig. 9A). Inactive E6AP had little effect on the core protein levels. Total protein levels in the cells (Fig. 9B) and intracellular HCV RNA levels (Fig. 9C) did not change after transfection of wild-type E6AP or inactive E6AP. The immunofluorescence study revealed that HCV core protein was variably detected and the intensity of core staining was reduced in the cells staining positive for wild-type E6AP compared with neighboring cells staining negative for E6AP (Fig. 9E). Using inactive E6AP revealed colocalization of the core protein and E6AP in the perinuclear region (Fig. 9F) of HCV-infected cells. These results suggest that E6AP enhanced degradation of HCV core protein expressed from infectious HCV. Then we titrated HCV infectivity in the culture supernatant at day 7 postinfection by limiting

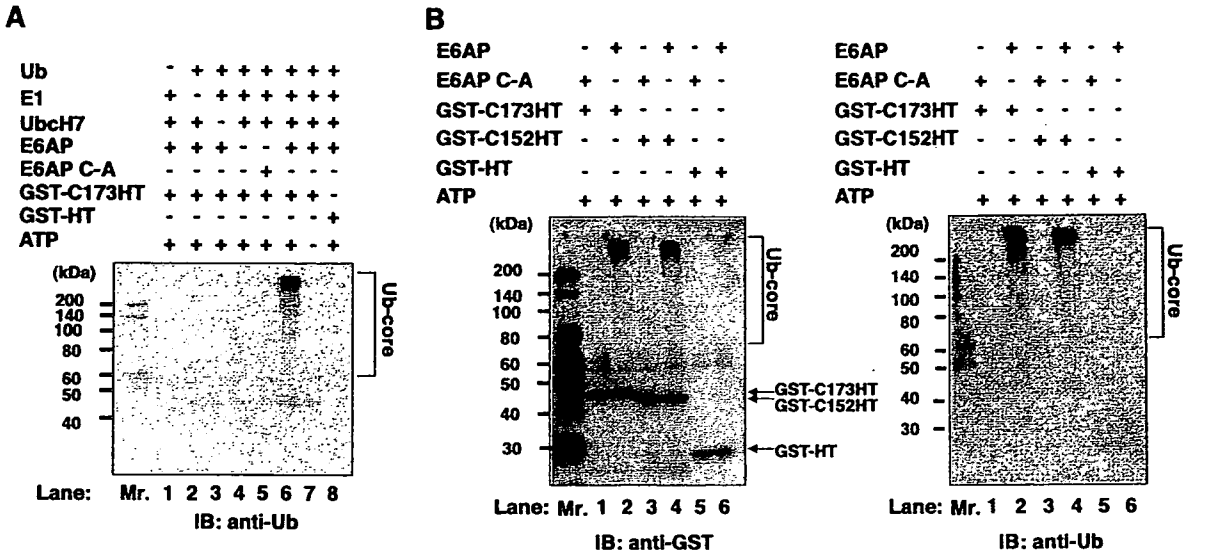

FIG. 8. In vitro ubiquitylation of HCV core protein by recombinant E6AP. For in vitro ubiquitylation of HCV core protein, purified GST-C173HT and GST-C152HT were used as substrates. Purified GST-HT was used as a negative control. Assays were done in 40-μl volumes containing each component as indicated. The reaction mixture is described in Materials and Methods. The reaction was carried out at 37°C for 120 min followed by purification with glutathione-Sepharose beads and analysis by immunoblotting with the indicated antibodies. Arrows indicate GST-C173HT, GST-C152HT, and GST-HT, respectively. Ubiquitylated species of GST-core proteins are marked by brackets. IB, immunoblot.

dilution assays. Exogenous expression of E6AP reduced the supernatant infectivity titer, whereas inactive E6AP had no effect on its infectivity titer (Fig. 9D), suggesting that the E6AP-dependent ubiquitin proteasome pathway affects the production of HCV particles through downregulation of the core protein.

E6AP silencing increases the levels of intracellular HCV core protein and supernatant infectivity titers in HCV-infected Huh-7 cells. Finally, to further validate the role of E6AP in HCV production, expression of endogenous E6AP was knocked down by siRNA and the HCV infectivity titers released from HCV JFH1-infected cells were examined. Knockdown of E6AP by siRNA led to an increase in intracellular core protein levels (Fig. 10A) and supernatant HCV infectivity titers (Fig. 10B). Taken together, our results suggest that E6AP mediates ubiquitylation and degradation of HCV core protein in HCV-infected cells, thereby affecting the production of HCV particles.

DISCUSSION

HCV core protein is a major component of viral nucleocapsid, plays a central role in viral assembly (25, 40), and contributes to viral pathogenesis and hepatocarcinogenesis (9). Therefore, it is important to clarify the molecular mechanisms that govern the cellular stability of this viral protein. We have previously reported that processing at the C-terminal hydrophobic domain of the core protein leads to efficient polyubiquitylation of the core protein (52). In this study, we identified E6AP as an HCV core-binding protein and showed that HCV core protein interacts with E6AP in vivo and in vitro, that E6AP enhances ubiquitylation and degradation of the mature core protein as well as the C-terminally truncated core protein, and that HCV core protein expressed from infectious HCV is degraded via E6AP-dependent proteolysis. HCV core protein and E6AP were found to colocalize in the cytoplasm, especially in the perinuclear region. Moreover, exogenous expression of E6AP reduces intracellular core protein levels and supernatant HCV infectivity titers in HCV-infected Huh-7 cells. Knockdown of endogenous E6AP by siRNA increases intracellular core protein levels and supernatant infectivity titers in HCV-infected cells. These findings suggest that E6AP mediates ubiquitylation and degradation of HCV core protein, thereby affecting the production of HCV particles.

HCV core protein interacts with E6AP through the region of the core protein between aa 58 and aa 71. These 14 amino acids are highly conserved, with the first nine amino acids (PRGRRQPIP) present in the core protein of all the HCV genotypes (3). This result suggests that E6AP-dependent degradation of HCV core protein is common to all HCV genotypes and plays an important role in the HCV life cycle or viral pathogenesis. Our data indicated that HCV core proteins of genotypes 1b and 2a are subjected to proteolysis through an E6AP-mediated degradation pathway. We are currently examining whether E6AP promotes degradation of HCV core proteins of other genotypes.

Studies in addition to ours have reported that other HCV proteins, such as NS5B (8), the unglycosylated cytosolic form of E2 (39), NS2 (7), and F protein (58), are degraded through the ubiquitin-proteasome pathway. These studies suggest that the ubiquitin-proteasome pathway plays a role in the HCV life cycle or viral pathogenesis. To our knowledge, the present study is the first to demonstrate that the ubiquitin-proteasome pathway affects the HCV life cycle.

PA28γ was found to interact with HCV core protein in hepatocytes and promote proteasomal degradation of HCV core protein (30). PA28γ, however, has been shown to function

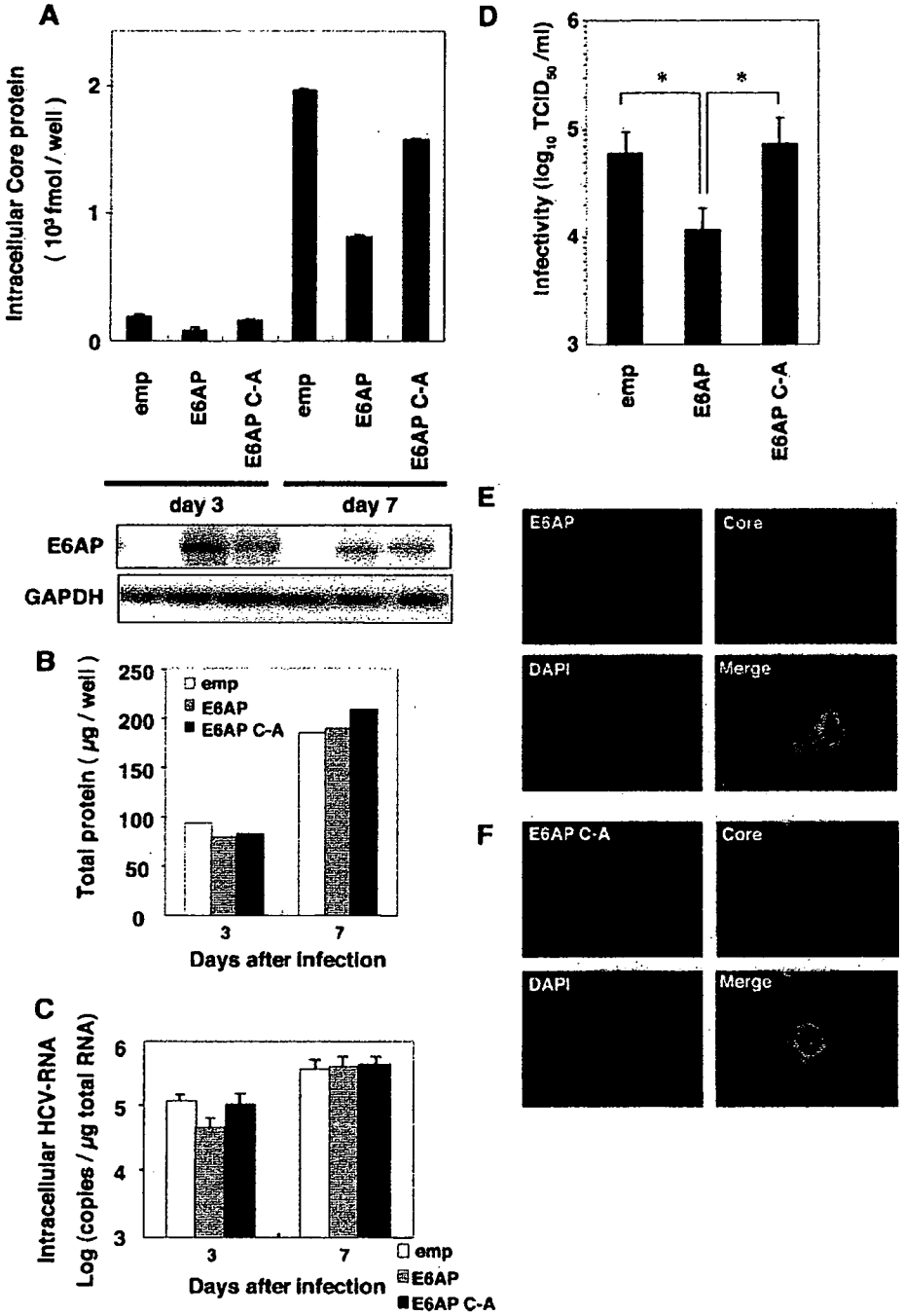

FIG. 9. Exogenous expression of E6AP reduces intracellular HCV core protein levels and supernatant infectivity titers in HCV-infected Huh-7 cells. Naïve Huh-7 cells were seeded as described in Materials and Methods; inoculated with 2.5 ml of the inoculum including infectious HCV JFH1 (6.5×10^3 $TCID_{50}$/ml); and transfected with 6 μg of empty plasmid, pCAG-HA-E6AP, or pCAG-HA-E6AP C-A. The culture supernatant and the cells were collected at days 3 and 7 postinfection. (A) Intracellular HCV core protein levels. (B) Levels of total protein. (C) Levels of intracellular HCV RNA in HCV-infected Huh-7 cells. Data represent the averages of three experiments with error bars. (D) Supernatant infectivity titers. At day 7 postinfection, culture supernatants were collected and assayed for $TCID_{50}$ determinations. The difference between empty vector and E6AP or between E6AP and E6AP C-A was significant (*, $P < 0.05$, Student's t test). (E and F) HCV JFH1-infected Huh-7 cells were transfected with either MEF-E6AP plasmid or MEF-E6AP C-A plasmid, grown on coverslips, fixed, and processed for double-label immunofluorescence for HCV core and MEF-E6AP (E) or MEF-E6AP C-A (F). Anticore MAb (2H9) and anti-FLAG PAb were used as primary antibodies. Nuclei were visualized by staining the cells with DAPI. All the samples were examined with a BZ-8000 microscope. Representative images of individual cells are shown with merge images. emp, empty vector.

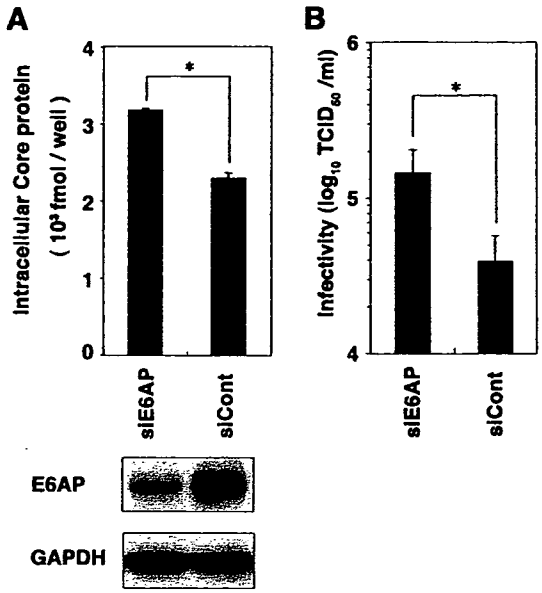

FIG. 10. E6AP silencing leads to an increase in the level of intracellular HCV core protein and supernatant infectivity titer in HCV-infected Huh-7 cells. (A) HCV JFH1-infected cells were replated in a six-well plate at 3×10^5 cells/well and transfected with 40 pmol of E6AP siRNA or control siRNA. The culture medium was changed at 24 h after transfection. The cells were harvested at day 2 after transfection, and the intracellular core protein levels were quantitated using the HCV core antigen ELISA. Equivalent amounts of the whole-cell lysates were separated by SDS-PAGE and analyzed by immunoblotting with anti-E6AP MAb or anti-GAPDH MAb. (B) Culture supernatants were collected at day 2 after transfection and assayed for $TCID_{50}$ determinations. For both panels, the difference between E6AP siRNA and control siRNA was significant (*, $P < 0.05$, Student's t test).

in a ubiquitin-independent, ATP-independent, and 20S proteasome-dependent pathway (27). There have been reports that several cellular factors, such as p53 (2), p73 (2), and RPN4 (18), are degraded through two alternative pathways, the ubiquitin-dependent 26S proteasome-dependent pathway and the ubiquitin-independent 20S proteasome-dependent pathway. Here we provide evidence that E6AP mediates ubiquitylation of HCV core protein. Still unclear is whether the PA28γ-dependent pathway requires polyubiquitylation of HCV core protein. HCV core protein is predominantly localized in the cytoplasm, especially at the endoplasmic reticulum membrane, on the surface of lipid droplets, and on mitochondria and mitochondrion-associated membranes (51). In HCV JFH1-infected cells, HCV core was found to localize in the cytoplasm and frequently to accumulate in the perinuclear region and the lipid droplets (44). Our results indicated that E6AP colocalized with HCV core protein especially in the perinuclear region. PA28γ was found to colocalize with HCV core protein in the nucleus. Functional differences may exist between the E6AP-dependent pathway and the PA28γ-dependent pathway in the stability control of HCV core protein. The functional role of the E6AP-dependent pathway and the PA28γ-dependent pathway remains to be elucidated.

The HCV core-binding region of E6AP was mapped to the region between aa 418 and aa 517. The multicopy maintenance protein 7, Mcm7, interacts with E6AP through a short motif, termed the L2G box (aa 412 to 414), that lies within the E6 binding site of E6AP (23). Our data indicated that the E6 binding region containing the L2G motif is not required for interaction between HCV core protein and E6AP (Fig. 2C, lane M).

We propose here that E6AP may affect the production of HCV particles through controlling the amounts of HCV core protein. This mechanism may contribute to persistent infection. The E6AP binding domain of the core protein resides in the RNA-binding domain and binding domains for many host factors (40). These factors may affect the binding between E6AP and HCV core protein, resulting in control of E6AP-dependent core degradation. Another possibility is that HCV core protein may affect the normal function of E6AP, thereby contributing to pathogenesis. It will be intriguing to investigate whether HCV core protein has any effect on E6AP-dependent degradation of host factors. The other intriguing possibility is that HCV core-E6AP complex may function as an E3 ligase-like E6-E6AP complex to target host factors for proteasomal degradation and contribute to viral pathogenesis.

In conclusion, we have demonstrated that E6AP interacts with HCV core protein in vitro and in vivo and mediates ubiquitin-dependent degradation of the core protein, leading to downregulation of HCV particles. We propose that the E6AP-mediated ubiquitin-proteasome pathway may play a role in affecting the production of HCV particles through controlling the amounts of viral nucleocapsid protein. Identification of the specific E3 ubiquitin ligase may contribute to gaining a better understanding of the biology of the HCV life cycle as well as molecular details of the ubiquitin-dependent degradation of HCV core protein.

ACKNOWLEDGMENTS

We thank D. Bohmann (EMBL) for providing pMT123, K. Miyazono (University of Tokyo) for pcDEF3-6Myc-WWP1, and K. Iwai (Osaka City University) for recombinant baculovirus carrying His 6-mouse E1. Huh-7.5.1 cells and Huh-7 cells were kindly provided by F. V. Chisari (Scripps Research Institute). We also thank P. Zhou (Weill Medical College of Cornell University), S. I. Wells (Cincinnati Children's Hospital Medical Center), and A. W. Hudson (Medical College of Wisconsin) for critical readings of the manuscript; M. Matsuda, S. Yoshizaki, M. Ikeda, and M. Sasaki for technical assistance; Y. Sugiyama and S. Senzui for plasmid construction; and T. Mizoguchi for secretarial work.

This work was supported in part by a grant for Research on Health Sciences focusing on Drug Innovation from the Japan Health Sciences Foundation; by grants-in-aid from the Ministry of Health, Labor and Welfare; by grants-in-aid from the Ministry of Education, Culture, Sports, Science and Technology; and by the program for Promotion of Fundamental Studies in Health Sciences of the National Institute of Biomedical Innovation (NIBIO), Japan. T.I. was supported in part by a grant from Novartis Foundation (Japan) for the Promotion of Science and by the Tokyo Metropolitan University President's Fund, Special Emphasis Research Project of Japan.

REFERENCES

1. **Aizaki, H., Y. Aoki, T. Harada, K. Ishii, T. Suzuki, S. Nagamori, G. Toda, Y. Matsuura, and T. Miyamura.** 1998. Full-length complementary DNA of hepatitis C virus genome from an infectious blood sample. Hepatology 27: 621–627.
2. **Asher, G., P. Tsvetkov, C. Kahana, and Y. Shaul.** 2005. A mechanism of ubiquitin-independent proteasomal degradation of the tumor suppressors p53 and p73. Genes Dev. 19:316–321.
3. **Bukh, J., R. H. Purcell, and R. H. Miller.** 1994. Sequence analysis of the core gene of 14 hepatitis C virus genotypes. Proc. Natl. Acad. Sci. USA 91:8239–8243.

4. **Chen, C., and H. Okayama.** 1987. High-efficiency transformation of mammalian cells by plasmid DNA. Mol. Cell. Biol. 7:2745–2752.
5. **Choo, Q. L., G. Kuo, A. J. Weiner, L. R. Overby, D. W. Bradley, and M. Houghton.** 1989. Isolation of a cDNA clone derived from a blood-borne non-A, non-B viral hepatitis genome. Science 244:359–362.
6. **Choo, Q. L., K. H. Richman, J. H. Han, K. Berger, C. Lee, C. Dong, C. Gallegos, D. Coit, R. Medina-Selby, P. J. Barr, et al.** 1991. Genetic organization and diversity of the hepatitis C virus. Proc. Natl. Acad. Sci. USA 88:2451–2455.
7. **Franck, N., J. Le Seyec, C. Guguen-Guillouzo, and L. Erdtmann.** 2005. Hepatitis C virus NS2 protein is phosphorylated by the protein kinase CK2 and targeted for degradation to the proteasome. J. Virol. 79:2700–2708.
8. **Gao, L., H. Tu, S. T. Shi, K. J. Lee, M. Asanaka, S. B. Hwang, and M. M. Lai.** 2003. Interaction with a ubiquitin-like protein enhances the ubiquitination and degradation of hepatitis C virus RNA-dependent RNA polymerase. J. Virol. 77:4149–4159.
9. **Giannini, C., and C. Brechot.** 2003. Hepatitis C virus biology. Cell Death Differ. 10(Suppl. 1):S27–S38.
10. **Grakoui, A., D. W. McCourt, C. Wychowski, S. M. Feinstone, and C. M. Rice.** 1993. Characterization of the hepatitis C virus-encoded serine proteinase: determination of proteinase-dependent polyprotein cleavage sites. J. Virol. 67:2832–2843.
11. **Harris, K. F., I. Shoji, E. M. Cooper, S. Kumar, H. Oda, and P. M. Howley.** 1999. Ubiquitin-mediated degradation of active Src tyrosine kinase. Proc. Natl. Acad. Sci. USA 96:13738–13743.
12. **Hijikata, M., H. Mizushima, T. Akagi, S. Mori, N. Kakiuchi, N. Kato, T. Tanaka, K. Kimura, and K. Shimotohno.** 1993. Two distinct proteinase activities required for the processing of a putative nonstructural precursor protein of hepatitis C virus. J. Virol. 67:4665–4675.
13. **Huibregtse, J. M., M. Scheffner, S. Beaudenon, and P. M. Howley.** 1995. A family of proteins structurally and functionally related to the E6-AP ubiquitin-protein ligase. Proc. Natl. Acad. Sci. USA 92:2563–2567.
14. **Huibregtse, J. M., M. Scheffner, and P. M. Howley.** 1993. Cloning and expression of the cDNA for E6-AP, a protein that mediates the interaction of the human papillomavirus E6 oncoprotein with p53. Mol. Cell. Biol. 13:775–784.
15. **Hussy, P., H. Langen, J. Mous, and H. Jacobsen.** 1996. Hepatitis C virus core protein: carboxy-terminal boundaries of two processed species suggest cleavage by a signal peptide peptidase. Virology 224:93–104.
16. **Ichimura, T., H. Yamamura, K. Sasamoto, Y. Tominaga, M. Taoka, K. Kakiuchi, T. Shinkawa, N. Takahashi, S. Shimada, and T. Isobe.** 2005. 14-3-3 proteins modulate the expression of epithelial Na^+ channels by phosphorylation-dependent interaction with Nedd4-2 ubiquitin ligase. J. Biol. Chem. 280:13187–13194.
17. **Iwai, K., K. Yamanaka, T. Kamura, N. Minato, R. C. Conaway, J. W. Conaway, R. D. Klausner, and A. Pause.** 1999. Identification of the von Hippel-Lindau tumor-suppressor protein as part of an active E3 ubiquitin ligase complex. Proc. Natl. Acad. Sci. USA 96:12436–12441.
18. **Ju, D., and Y. Xie.** 2004. Proteasomal degradation of RPN4 via two distinct mechanisms, ubiquitin-dependent and -independent. J. Biol. Chem. 279: 23851–23854.
19. **Kao, W. H., S. L. Beaudenon, A. L. Talis, J. M. Huibregtse, and P. M. Howley.** 2000. Human papillomavirus type 16 E6 induces self-ubiquitination of the E6AP ubiquitin-protein ligase. J. Virol. 74:6408–6417.
20. **Kato, T., M. Miyamoto, A. Furusaka, T. Date, K. Yasui, J. Kato, S. Matsushima, T. Komatsu, and T. Wakita.** 2003. Processing of hepatitis C virus core protein is regulated by its C-terminal sequence. J. Med. Virol. 69:357–366.
21. **Kishino, T., M. Lalande, and J. Wagstaff.** 1997. UBE3A/E6-AP mutations cause Angelman syndrome. Nat. Genet. 15:70–73.
22. **Komuro, A., T. Imamura, M. Saitoh, Y. Yoshida, T. Yamori, K. Miyazono, and K. Miyazawa.** 2004. Negative regulation of transforming growth factor-beta (TGF-beta) signaling by WW domain-containing protein 1 (WWP1). Oncogene 23:6914–6923.
23. **Kuhne, C., and L. Banks.** 1998. E3-ubiquitin ligase/E6-AP links multicopy maintenance protein 7 to the ubiquitination pathway by a novel motif, the L2G box. J. Biol. Chem. 273:34302–34309.
24. **Kumar, S., A. L. Talis, and P. M. Howley.** 1999. Identification of HHR23A as a substrate for E6-associated protein-mediated ubiquitination. J. Biol. Chem. 274:18785–18792.
25. **Kunkel, M., M. Lorinczi, R. Rijnbrand, S. M. Lemon, and S. J. Watowich.** 2001. Self-assembly of nucleocapsid-like particles from recombinant hepatitis C virus core protein. J. Virol. 75:2119–2129.
26. **Kuo, G., Q. L. Choo, H. J. Alter, G. L. Gitnick, A. G. Redeker, R. H. Purcell, T. Miyamura, J. L. Dienstag, M. J. Alter, C. E. Stevens, et al.** 1989. An assay for circulating antibodies to a major etiologic virus of human non-A, non-B hepatitis. Science 244:362–364.
27. **Li, X., D. M. Lonard, S. Y. Jung, A. Malovannaya, Q. Feng, J. Qin, S. Y. Tsai, M. J. Tsai, and B. W. O'Malley.** 2006. The SRC-3/AIB1 coactivator is degraded in a ubiquitin- and ATP-independent manner by the REGγ proteasome. Cell 124:381–392.
28. **Lindenbach, B. D., M. J. Evans, A. J. Syder, B. Wolk, T. L. Tellinghuisen, C. C. Liu, T. Maruyama, R. O. Hynes, D. R. Burton, J. A. McKeating, and C. M. Rice.** 2005. Complete replication of hepatitis C virus in cell culture. Science 309:623–626.
29. **McLauchlan, J., M. K. Lemberg, G. Hope, and B. Martoglio.** 2002. Intramembrane proteolysis promotes trafficking of hepatitis C virus core protein to lipid droplets. EMBO J. 21:3980–3988.
30. **Moriishi, K., T. Okabayashi, K. Nakai, K. Moriya, K. Koike, S. Murata, T. Chiba, K. Tanaka, R. Suzuki, T. Suzuki, T. Miyamura, and Y. Matsuura.** 2003. Proteasome activator PA28γ-dependent nuclear retention and degradation of hepatitis C virus core protein. J. Virol. 77:10237–10249.
31. **Moriya, K., H. Fujie, Y. Shintani, H. Yotsuyanagi, T. Tsutsumi, K. Ishibashi, Y. Matsuura, S. Kimura, T. Miyamura, and K. Koike.** 1998. The core protein of hepatitis C virus induces hepatocellular carcinoma in transgenic mice. Nat. Med. 4:1065–1067.
32. **Moriya, K., H. Yotsuyanagi, Y. Shintani, H. Fujie, K. Ishibashi, Y. Matsuura, T. Miyamura, and K. Koike.** 1997. Hepatitis C virus core protein induces hepatic steatosis in transgenic mice. J. Gen. Virol. 78:1527–1531.
33. **Natsume, T., Y. Yamauchi, H. Nakayama, T. Shinkawa, M. Yanagida, N. Takahashi, and T. Isobe.** 2002. A direct nanoflow liquid chromatography-tandem mass spectrometry system for interaction proteomics. Anal. Chem. 74:4725–4733.
34. **Niwa, H., K. Yamamura, and J. Miyazaki.** 1991. Efficient selection for high-expression transfectants with a novel eukaryotic vector. Gene 108:193–199.
35. **Oda, H., S. Kumar, and P. M. Howley.** 1999. Regulation of the Src family tyrosine kinase Blk through E6AP-mediated ubiquitination. Proc. Natl. Acad. Sci. USA 96:9557–9562.
36. **Ogino, T., H. Fukuda, S. Imajoh-Ohmi, M. Kohara, and A. Nomoto.** 2004. Membrane binding properties and terminal residues of the mature hepatitis C virus capsid protein in insect cells. J. Virol. 78:11766–11777.
37. **Okamoto, K., K. Moriishi, T. Miyamura, and Y. Matsuura.** 2004. Intramembrane proteolysis and endoplasmic reticulum retention of hepatitis C virus core protein. J. Virol. 78:6370–6380.
38. **Owsianka, A. M., and A. H. Patel.** 1999. Hepatitis C virus core protein interacts with a human DEAD box protein DDX3. Virology 257:330–340.
39. **Pavio, N., D. R. Taylor, and M. M. Lai.** 2002. Detection of a novel unglycosylated form of hepatitis C virus E2 envelope protein that is located in the cytosol and interacts with PKR. J. Virol. 76:1265–1272.
40. **Polyak, S. J., K. C. Klein, I. Shoji, T. Miyamura, and J. R. Lingappa.** 2006. Assemble and interact: pleiotropic functions of the HCV core protein, p. 89–119. *In* S.-L. Tan (ed.), Hepatitis C viruses: genomes and molecular biology. Horizon Bioscience, Norwich, United Kingdom.
41. **Poynard, T., M. F. Yuen, V. Ratziu, and C. L. Lai.** 2003. Viral hepatitis C. Lancet 362:2095–2100.
42. **Ravaggi, A., G. Natoli, D. Primi, A. Albertini, M. Levrero, and E. Cariani.** 1994. Intracellular localization of full-length and truncated hepatitis C virus core protein expressed in mammalian cells. J. Hepatol. 20:833–836.
43. **Ray, R. B., L. M. Lagging, K. Meyer, and R. Ray.** 1996. Hepatitis C virus core protein cooperates with *ras* and transforms primary rat embryo fibroblasts to tumorigenic phenotype. J. Virol. 70:4438–4443.
44. **Rouille, Y., F. Helle, D. Delgrange, P. Roingeard, C. Voisset, E. Blanchard, S. Belouzard, J. McKeating, A. H. Patel, G. Maertens, T. Wakita, C. Wychowski, and J. Dubuisson.** 2006. Subcellular localization of hepatitis C virus structural proteins in a cell culture system that efficiently replicates the virus. J. Virol. 80:2832–2841.
45. **Saito, I., T. Miyamura, A. Ohbayashi, H. Harada, T. Katayama, S. Kikuchi, Y. Watanabe, S. Koi, M. Onji, Y. Ohta, et al.** 1990. Hepatitis C virus infection is associated with the development of hepatocellular carcinoma. Proc. Natl. Acad. Sci. USA 87:6547–6549.
46. **Santolini, E., G. Migliaccio, and N. La Monica.** 1994. Biosynthesis and biochemical properties of the hepatitis C virus core protein. J. Virol. 68: 3631–3641.
47. **Sato, S., M. Fukasawa, Y. Yamakawa, T. Natsume, T. Suzuki, I. Shoji, H. Aizaki, T. Miyamura, and M. Nishijima.** 2006. Proteomic profiling of lipid droplet proteins in hepatoma cell lines expressing hepatitis C virus core protein. J. Biochem. (Tokyo) 139:921–930.
48. **Scheffner, M., J. M. Huibregtse, and P. M. Howley.** 1994. Identification of a human ubiquitin-conjugating enzyme that mediates the E6-AP-dependent ubiquitination of p53. Proc. Natl. Acad. Sci. USA 91:8797–8801.
49. **Scheffner, M., J. M. Huibregtse, R. D. Vierstra, and P. M. Howley.** 1993. The HPV-16 E6 and E6-AP complex functions as a ubiquitin-protein ligase in the ubiquitination of p53. Cell 75:495–505.
50. **Scheffner, M., U. Nuber, and J. M. Huibregtse.** 1995. Protein ubiquitination involving an E1-E2-E3 enzyme ubiquitin thioester cascade. Nature 373:81–83.
51. **Suzuki, R., S. Sakamoto, T. Tsutsumi, A. Rikimaru, K. Tanaka, T. Shimoike, K. Moriishi, T. Iwasaki, K. Mizumoto, Y. Matsuura, T. Miyamura, and T. Suzuki.** 2005. Molecular determinants for subcellular localization of hepatitis C virus core protein. J. Virol. 79:1271–1281.
52. **Suzuki, R., K. Tamura, J. Li, K. Ishii, Y. Matsuura, T. Miyamura, and T. Suzuki.** 2001. Ubiquitin-mediated degradation of hepatitis C virus core pro-

Available online at www.sciencedirect.com
SCIENCE DIRECT
VIROLOGY
Virology 351 (2006) 381–392
www.elsevier.com/locate/yviro

Production of infectious hepatitis C virus particles in three-dimensional cultures of the cell line carrying the genome-length dicistronic viral RNA of genotype 1b

Kyoko Murakami [a], Koji Ishii [a], Yousuke Ishihara [b], Sayaka Yoshizaki [a], Keiko Tanaka [c], Yasufumi Gotoh [d,e], Hideki Aizaki [a], Michinori Kohara [f], Hiroshi Yoshioka [g], Yuichi Mori [g], Noboru Manabe [d], Ikuo Shoji [a], Tetsutaro Sata [c], Ralf Bartenschlager [h], Yoshiharu Matsuura [i], Tatsuo Miyamura [a], Tetsuro Suzuki [a,*]

[a] *Department of Virology II, National Institute of Infectious Diseases, 1-23-1 Toyama, Shinjuku-ku, Tokyo 162-8640, Japan*
[b] *Hanaichi Ultrastructure Research Institute, Okazaki, Aichi 444-0076, Japan*
[c] *Department of Pathology, National Institute of Infectious Diseases, Shinjuku, Tokyo 162-8640, Japan*
[d] *Research Unit for Animal Life Sciences, Animal Resource Science Center, The University of Tokyo, Iwama, Ibaraki 319-0206, Japan*
[e] *Unit of Anatomy and Cell Biology, Department of Animal Sciences, Kyoto University, Kyoto 606-8502, Japan*
[f] *Department of Microbiology and Cell Biology, Tokyo Metropolitan Institute of Medical Science, Bunkyo-ku, Tokyo 113-8613, Japan*
[g] *Mebiol Inc., Hiratsuka, Kanagawa 254-0075, Japan*
[h] *Department of Molecular Virology, Hygiene Institute, University Heidelberg, Im Neuenhemier Feld 345, D-69120 Heidelberg, Germany*
[i] *Department of Molecular Virology, Research Institute for Microbial Diseases, Osaka University, Suita, Osaka 565-0871, Japan*

Received 5 January 2006; returned to author with revision 23 January 2006; accepted 24 March 2006
Available online 6 May 2006

Abstract

We show that a dicistronic hepatitis C virus (HCV) genome of genotype 1b supports the production and secretion of infectious HCV particles in two independent three-dimensional (3D) culture systems, the radial-flow bioreactor and the thermoreversible gelation polymer (TGP), but not in monolayer cultures. Immunoreactive enveloped particles, which are 50–60 nm in diameter and are surrounded by membrane-like structures, are observed in the culture medium as well as at the endoplasmic reticulum membranes and in dilated cytoplasmic cisternae in spheroids of Huh-7 cells. Infection of HCV particles is neutralized by anti-E2 antibody or patient sera that interfere with E2 binding to human cells. Finally, the utility of the 3D-TGP culture system for the evaluation of antiviral drugs is shown. We conclude that the replicon-based 3D culture system allows the production of infectious HCV particles. This system is a valuable tool in studies of HCV morphogenesis in a natural host cell environment.

Keywords: Hepatitis C virus; Replication; Three-dimensional culture; Virus particle

Introduction

Infection with hepatitis C virus (HCV) currently represents a major medical and socioeconomic problem. HCV is a main causative agent of chronic hepatitis, cirrhosis, and hepatocellular carcinoma, and there are an estimated 170 million HCV carriers worldwide (Choo et al., 1989). The standard treatments for HCV infection are interferon alpha (IFN-α) in combination with ribavirin (RBV) or, more recently, a polyethylene glycol-modified form of IFN-α; however, sustained response is seen in only ~50% of treated patients (Davis et al., 2003; Manns et al., 2001). Further development of new anti-HCV drugs and vaccines has been obstructed by the lack of either a small animal model or a robust cell culture system capable of supporting viral replication and the production of infectious progeny.

HCV is a small enveloped RNA virus belonging to the family Flaviviridae and harboring a single-stranded RNA genome with

* Corresponding author. Fax: +81 3 5285 1161.
E-mail address: tesuzuki@nih.go.jp (T. Suzuki).

0042-6822/$ - see front matter © 2006 Elsevier Inc. All rights reserved.
doi:10.1016/j.virol.2006.03.038

positive polarity. A precursor polyprotein of ~3000 amino acids (aa) is encoded by a large open reading frame. This polyprotein is cleaved by cellular and viral proteases to give rise to a series of structural and nonstructural proteins (Choo et al., 1991; Grakoui et al., 1993; Hijikata et al., 1991). The establishment of selectable dicistronic HCV RNAs that are capable of autonomous replication in human hepatoma Huh-7 cells was a significant breakthrough in HCV research (Blight et al., 2000; Lohmann et al., 1999) and has provided an important tool for the study of HCV replication mechanisms and for screening antiviral drugs (Frese et al., 2001; Guo et al., 2001). This replicon system was first developed to replicate only viral subgenomic RNAs but has been further expanded to enable the replication of genome-length dicistronic RNAs (Ikeda et al., 2002; Pietschmann et al., 2002). Although the viral genome replicates and all HCV proteins are properly processed in this system, virus particle production has not yet been achieved. A number of researchers (Date et al., 2004; Kato et al., 2001, 2003) have developed an HCV genotype 2a replicon (JFH-1) that efficiently replicates in a variety of human cells. Recently, it has been demonstrated that the full-length JFH-1 genome or a chimeric genome using JFH-1 and J6, a related genotype 2a strain, produces infectious particles in cell cultures (Lindenbach et al., 2005; Wakita et al., 2005; Zhong et al., 2005). More recently, production of infectious genotype 1a virus (Hutchinson strain) using similar experimental systems has been described (Yi et al., 2006). These complete HCV culture systems produce robust levels of infectious virus and provides a powerful tool for HCV research. However, to date their applications have not been extended to constructs based on strains of genotype 1b, which is highly prevalent worldwide.

We previously demonstrated that differentiated human hepatoma FLC4 cells transfected with in vitro transcribed HCV genomic RNA can produce and secrete infectious particles in three-dimensional (3D) radial-flow bioreactor (RFB) culture (Aizaki et al., 2003). This RFB system was initially aimed to develop artificial liver tissue, and the bioreactor column consists of a vertically extended cylindrical matrix through which liquid medium flows continuously from the periphery toward the center of the reactor (Kawada et al., 1998). In RFB culture, human hepatocellular carcinoma-derived cells can grow spherically or cubically, and they retain liver functions such as albumin synthesis (Kawada et al., 1998; Matsuura et al., 1998) and drug-metabolizing activity mediated by cytochrome P450 3A4 (Iwahori et al., 2003).

In the present study, two kinds of 3D culture techniques, the RFB and the thermoreversible gelation polymer (TGP), were used for the production and secretion of infectious HCV particles by using a dicistronic HCV genome derived from genotype 1b. We also demonstrate that these 3D culture systems are useful for evaluating anti-HCV drugs.

Results

Secretion of HCV-LPs from RCYM1 carrying genome-length dicistronic HCV RNA cultured in RFB culture

We first assessed the replicative capacity of selectable genome-length HCV RNAs in FLC4 cells. However, no G418-resistant colonies were observed, indicating that FLC4 cells do not support replication of these HCV RNAs (data not shown). Therefore, subsequent experiments were carried out with a stable Huh-7 cell line, RCYM1, which supports full-length HCV RNA replication and which was developed by transfection of the cells with genome-length dicistronic RNA derived from the Con1 clone I389neo/core-3′/NK 5.1 (genotype 1b)

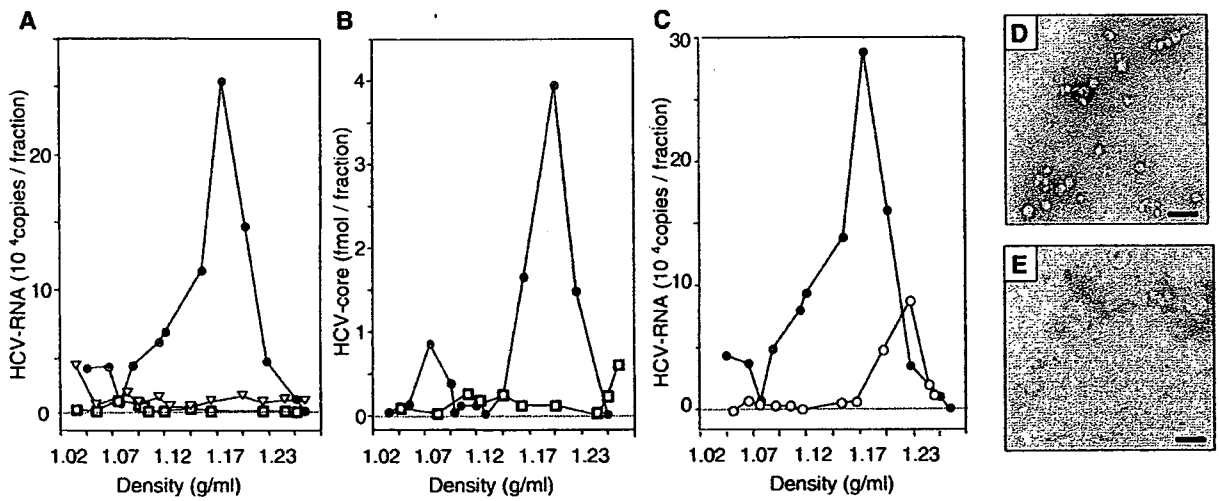

Fig. 1. Sucrose density gradient analysis of culture supernatants of RCYM1 cells. Culture media collected from radial-flow bioreactor (RFB)-cultured RCYM1 (closed circles), monolayer-cultured RCYM1 (open squares), and RFB-cultured 5–15 cells (open triangles) were fractionated as described in Materials and methods. (A) HCV RNA in each fraction was measured by real-time reverse transcriptase-polymerase chain reaction (RT-PCR). Mean values of duplicates were plotted against the density of the corresponding fraction. (B) HCV core protein in each fraction was determined by enzyme-linked immunosorbent assay (ELISA). Mean values of duplicates were plotted against the density. (C) Culture medium of RFB-cultured RCM1 cells were treated with 0.2% NP40 (open circles), followed by centrifugation in a sucrose gradient. Each fraction was tested for HCV RNA by real-time RT-PCR. (D, E) Electron microscopy analysis. Samples were prepared from the 1.18 g/ml fraction of culture media collected from RFB-cultured (D) or monolayer-cultured (E) RCYM1 cells.

(Pietschmann et al., 2002). The HCV RNA level in RCYM1 cells was approximately 5 × 10^6 copies/μg total RNA as determined by real-time reverse transcriptase-polymerase chain reaction (RT-PCR). The expression and subcellular localization of HCV protein were confirmed by Western blotting and immunofluorescence analysis (data not shown). To develop 3D RFB cultures, first we loaded RCYM1 cells onto an RFB column by flowing cell suspension, after which the cells were attached to carrier beads. Cells proliferated within the 3D matrix, and culture medium was circulated radially through the column.

In order to investigate whether HCV-like particles (HCV-LPs) were secreted from RCYM1 cells in the RFB culture system, we fractionated culture fluid collected after 5–10 days of culture by continuous 10–60% (wt/vol) sucrose density gradient centrifugation. HCV RNA and core protein were predominantly detected in the 1.15–1.20 g/ml fractions, with maximal detection in the 1.18 g/ml fraction (Figs. 1A and B). In the same experiment using 5–15 cells, in which a subgenomic HCV replicon replicates, no peak similar to that observed in RCYM1 cells corresponding to HCV RNA was detected. In both RCYM1 cells and 5–15 cells in the RFB culture system, a substantial amount of HCV RNA was detected in the 1.03–1.07 g/ml fractions (Fig. 1A). Consistent with a previous report by Pietschmann et al. (2002), these RNAs released from cells with a subgenomic replicon did not correspond to virus particles. When an equivalent number of RCYM1 cells were cultured in a monolayer culture system, limited amounts of HCV RNA and core protein were detected in the culture supernatant (Figs. 1A and B).

The mature HCV virion is thought to have a nucleocapsid and an outer envelope composed of a lipid membrane with viral envelope glycoproteins. Culture fluids were treated with NP40 in order to solubilize lipids and were then subjected to sucrose density gradient centrifugation. HCV RNA sedimented to a density of 1.22 g/ml rather than 1.18 g/ml (Fig. 1C), indicating that the density of HCV particles became higher due to de-envelopment. Transmission electron microscopy (TEM) of the 1.18 g/ml fraction, which was subjected to negative staining after concentration, revealed particle structures with diameters of 30–60 nm and a major particle size of 50 nm (Fig. 1D). No similar particle-like structures were observed in the same density fraction of the RCYM1 monolayer culture (Fig. 1E) or in the 1.23 g/ml fraction of the RCYM1-RFB culture (data not shown). These results indicate that, in the RFB system, the production and secretion of HCV-LPs is possible with a selectable dicistronic HCV genome.

Production and secretion of HCV-LPs from spheroid culture of RCYM1 cells using TGP

In the 3D RFB culture system for RCYM1 cells, extracellular secretion of HCV-LPs was observed. Based on this observation, we hypothesized that morphological changes occurring in 3D culture, such as polarity formation, promote advantageous in the assembly of viral proteins, particle formation, and extracellular secretion. To examine whether similar phenomena could be observed in other 3D culture systems, we investigated HCV-LP expression using a 3D culture system with TGP as a carrier.

TGP is a biocompatible polymer made from conjugates of polyethyleneglycol and poly-*N*-isopropylacrylamide, which is a thermoresponsive polymer composed of *N*-isopropylacrylamide and *n*-butylmethacrylate. The TGP solution possesses sol-gel transition properties; it is water soluble (sol phase) at temperatures below the transition temperature, and it is insoluble (gel phase) above it. It is possible to manipulate the transition temperatures through molecular engineering. The transition temperature for TGP in the present experiments was approximately 20 °C.

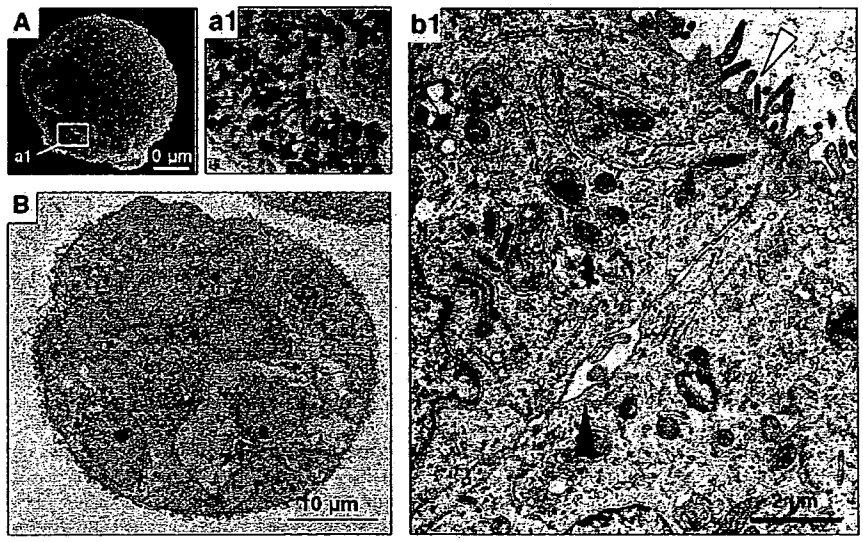

Fig. 2. Huh-7 and RCYM1 cells form spheroids in thermoreversible gelation polymer (TGP). Scanning electron microscopy (A and a1) and transmission electron microscopy (B and b1) of RCYM1 cells cultured in TGP for 8 days. Open arrowhead, microvilli; closed arrowheads, bile canaliculi-like structures.

RCYM1 cells, which were seeded into the TGP, formed three-dimensional compacted aggregates called spheroids after 3 days of culture, and numerous spheroids with diameters of approximately 1 mm were observed after 7–10 days of culture. After 8 days of culture, the spheroids were fixed and examined by scanning electron microscopy (Figs. 2A and a1) and ultrathin sections were examined by TEM (Figs. 2B and b1). Well-developed microvilli, a feature of polarized epithelium, were observed on the cell surface (Figs. 2A and a1). Bile canaliculi-like structures were also observed within intercellular spaces, and they appeared to be connected via tight junctions (Figs. 2B and b1). This cytomorphology, similar to that observed in the RFB culture (Kawada et al., 1998; Matsuura et al., 1998), correlated well with the features of mature liver tissue.

It is known that the replication of HCV replicons in Huh-7 cells depends on host cell growth. We found that the growth of RCYM1 cells in the TGP culture system was significantly slower than that of cells in monolayer culture (Fig. 3A). Accordingly, the expression of HCV proteins (Fig. 3B) in the RCYM1 spheroids was apparently lower compared to those observed in the monolayer cells. The viral RNA copy number in the spheroids was approximately one tenth of that in the monolayer culture (data not shown). The results of sucrose density gradient analysis of culture supernatant demonstrated co-sedimentation of HCV RNAs and core proteins at a density of 1.15–1.20 g/ml, with a peak at 1.18 g/ml (Figs. 3C and D). This distribution was consistent with the pattern obtained in RFB culture (Figs. 1A and B). It should be noted that in these experiments, lower cell numbers were used in the 3D cultures than in the monolayer cultures because of the slower growth of cells. As estimated from the quantitative data of the 1.15–1.20 g/ml fractions of the culture supernatants, 0.1–1 copies of HCV RNA/cell/day are produced and assembled into viral particles in the TGP-cultured RCYM1 cells.

TEM analysis of the 1.18 g/ml fraction after negative staining showed particle structures with a diameter of 50–60 nm and spike-like projections (Fig. 3E). Observation of ultrathin sections indicated a lipid bilayer-like membrane structure with a

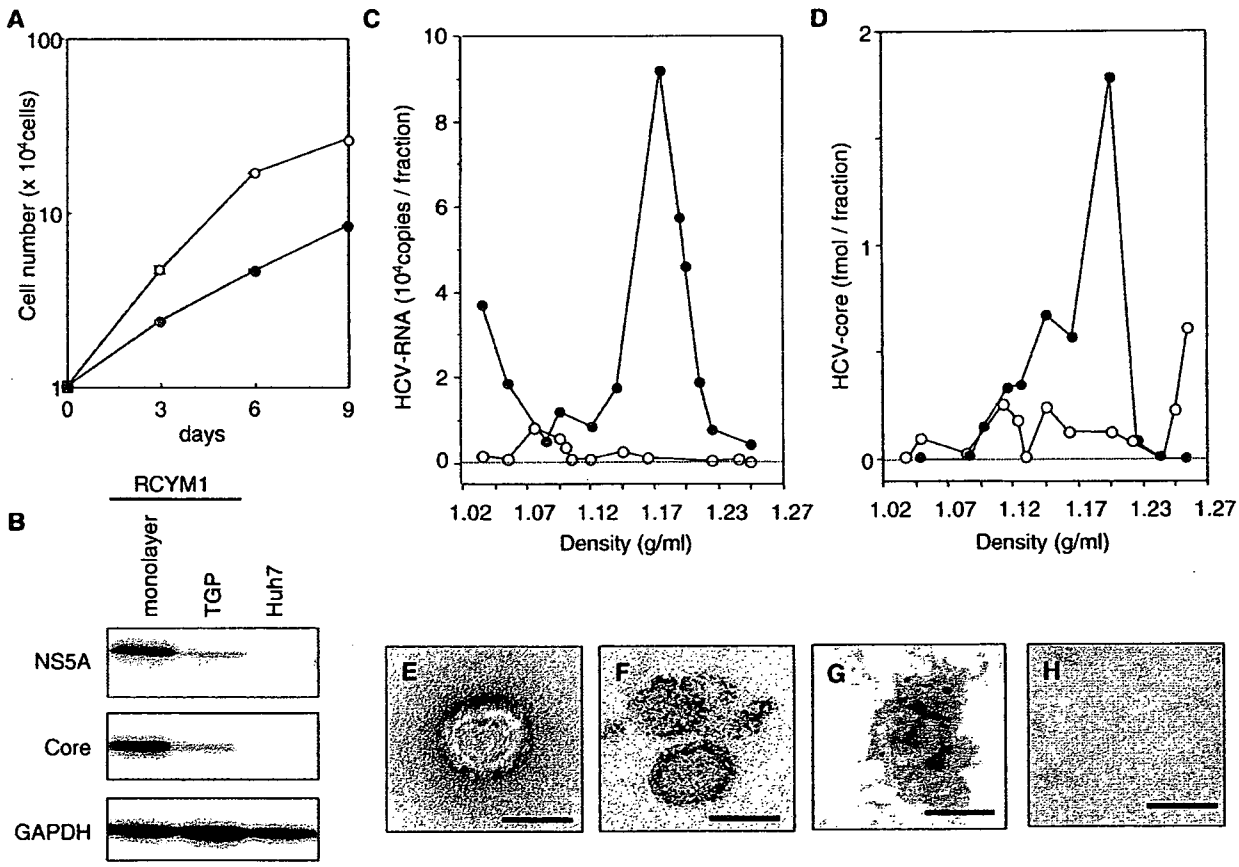

Fig. 3. Expression of HCV proteins in RCYM1 cells and secretion of viral particles in TGP culture. (A) Cell growth curves of the TGP (closed circles) and monolayer (open circles) culture of RCYM1 cells. Cells were harvested at days 0, 3, 6, and 9 postinoculation and cell numbers were determined. (B) Western blotting of HCV core and NS5A proteins in RCYM1 cells and control Huh-7 cells. (C, D) Sucrose density gradient analysis of culture supernatants of RCYM1 cells. The culture supernatants were fractionated as described in Materials and methods. HCV RNA (C) and core protein (D) in each fraction were determined by ELISA and real-time RT-PCR, respectively. Representative data from three independent experiments are shown. Closed circles, TGP culture; open circles, monolayer culture. (E–H) Electron microscopy of HCV-like particles (HCV-LPs) in the supernatants of TGP-cultured RCYM1 cells. (E) Negative staining of HCV-LPs in the 1.18 g/ml density fraction. There was no spherical structure in 1.05 g/ml density fraction, as shown in panel H. (F) Ultrathin section of HCV-LPs. Precipitated HCV-LP samples were prepared from the 1.18 g/ml fraction as described in Materials and methods. (G) Immunogold labeling of HCV-LPs with an anti-E2 antibody in the 1.18 g/ml density fraction. Gold particles, 5 nm; scale bars, 50 nm.

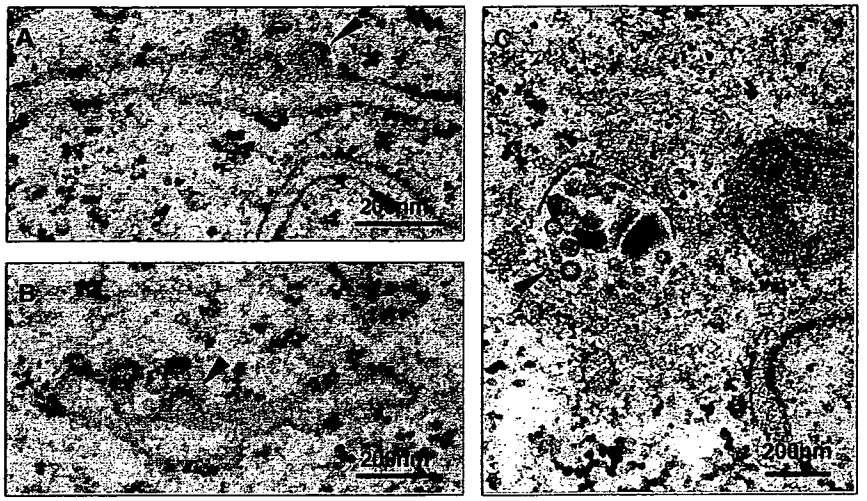

Fig. 4. Electron microscopy of ultrathin sections of RCYM1 cells grown in TGP. HCV-LPs in TGP-cultured RCYM1 cells. Spherical virus-like particles 50–60 nm in diameter (arrowheads) were observed at the ER membranes (A, B) and in the cytoplasmic vesicles (C).

width of approximately 5 nm (Fig. 3F). Immunoelectron microscopic study using anti-E2 antibody revealed HCV envelope protein(s) on the particle surface (Fig. 3G). Substantial amounts of HCV RNA were detected in the 1.03–1.05 g/ml fractions of the supernatant (Fig. 3C); however, HCV-LP structures were not observed in these fractions (Fig. 3H). These results were consistent with those from the RFB system, as shown above. The efficacy of 3D cell culture systems in virion formation was thus demonstrated in both the RFB and TGP culture systems using human liver-derived cells.

Ultrastructural localization of HCV-LPs in TGP-cultured spheroids of RCYM1 cells

We next determined the intracellular localization of HCV-LPs produced in RCYM1-TGP culture at the ultrastructural level by electron microscopic (EM) analysis of ultrathin sections. Spherical particles having membrane-like structures with short surface projections (diameter, 50–60 nm) were observed primarily at the endoplasmic reticulum (ER) membrane (Fig. 4A) as well as in the dilated cisternae of the ER (Fig. 4B). In vesicles, these virus-like particles were frequently associated with amorphous materials (Fig. 4C). In a previous study, Shimizu et al. (1996) report that virus-like particles with similar morphology and size were observed in human B cells infected with HCV. No similar particle-like structures were observed in RCYM1 cells in monolayer culture or in subgenomic replicon 5–15 in cells in TGP culture (data not shown).

In order to determine whether the virus-like particles observed by conventional TEM in the present experiment were HCV-LPs, we conducted immunoelectron microscopic analysis with anti-core antibody and anti-E1 antibody. Double-labeling experiments showed that the virus-like particles associated with the ER membrane exhibited immunoreactivity for both HCV proteins, and that the E1 protein surrounded the core proteins (Fig. 5A). To the best of our knowledge, this is the first report to clearly demonstrate that the viral envelope protein surrounds the core protein in HCV particle formation. As a negative control, thin sections prepared from subgenomic RNA containing 5–15 cells were stained with these antibodies and were found to exhibit negligible levels of background immunostaining (data not shown).

Fig. 5. Immunoelectron microscopy of ultrathin sections of TGP-cultured RCYM1 cells. (A) Double immunostaining with anti-E1 and anti-core monoclonal antibodies. Core protein-specific gold particles (10 nm in diameter) and E1 protein-specific gold particles (5 nm in diameter) formed rosettes on the surface of the ER membrane. (B and C) Silver-intensified immunogold staining with anti-core (B) and anti-E1 (C) antibodies. The second antibody conjugated with gold particles 1.4 nm in diameter was applied, followed by enlargement of the particles by the silver enhancement reagent. Arrowheads indicate virus-like particles reacting with anti-core and/or anti-E1 antibodies.

It is generally difficult to visualize intracellular microstructures and perform antigenic protein localizations using immunogold electron microscopy due to the low resolution and contrast of micrographs. In order to overcome this difficulty, we applied a silver-intensified immunogold labeling method in our experiment (Figs. 5B and C). Using this method, antigen-reactive immunogold particles approximately 20 nm in diameter were observed. Specific immunolabeling of core and E1 protein was detected in the ER or on the ER membranes. Intense immunopositive reactions were also seen on the virus-like particles observed in cytoplasmic vesicles and on ER membranes; however, no such immunolabeling was observed when normal mouse serum was used as a first antibody (data not shown). These results confirm the ultrastructural observations of conventional TEM and suggest that the formation of HCV particles is achieved by budding of the putative core particles at the ER membrane.

Infectivity of HCV-LPs depends on E2 glycoprotein

To determine whether HCV-LPs released from RCYM1 cells cultured in the TGP system are infectious, we inoculated naive Huh-7.5.1 cells (Zhong et al., 2005), which are HCV-negative Huh-7.5 (Blight et al., 2002)-derived cells, with a culture supernatant of RCYM1 spheroids. HCV RNAs in the cells at days 0, 1, 2, 3, and 7 postinoculation were determined by real-time RT-PCR. Fig. 6A shows the kinetics of HCV RNA after the inoculation of HCV-LPs. HCV RNA levels in the infected Huh-7.5.1 cells fluctuated at the indicated times, reaching 10^3–10^4 copies/μg of cellular RNA at days 1–7. Immunofluorescence staining 4 days postinoculation revealed that approximately 1% of cells were positive for NS5A protein (Fig. 6B). In contrast, no NS5A-positive cells were detected when the cell supernatant sample obtained from 5 to 15 cell cultured in TGP was used to inoculate Huh-7.5.1 cells (data not shown). These results suggest that HCV-LPs released from TGP-cultured RCYM1 cells are infectious.

To further determine whether viral envelope proteins mediate infection by HCV-LPs, we preincubated HCV-LPs with the anti-E2 monoclonal antibody AP33, which demonstrates potent neutralization of infectivity against HCV pseudoparticles carrying E1 and E2 proteins representative of the major genotypes 1 through 6 (Owsianka et al., 2005), or with patient sera with high titers of HCV neutralization of binding (NOB) antibodies (Ishii et al., 1998), or with anti-FLAG antibody (Fig. 6C). NOB antibodies have the ability to neutralize the binding of E2 protein to human cells (Rosa et al., 1996), and NOB3 and NOB4 were sera obtained from patients who recovered naturally from chronic hepatitis C (Ishii et al., 1998). Intracellular HCV RNA levels were decreased by 43%, 28%,

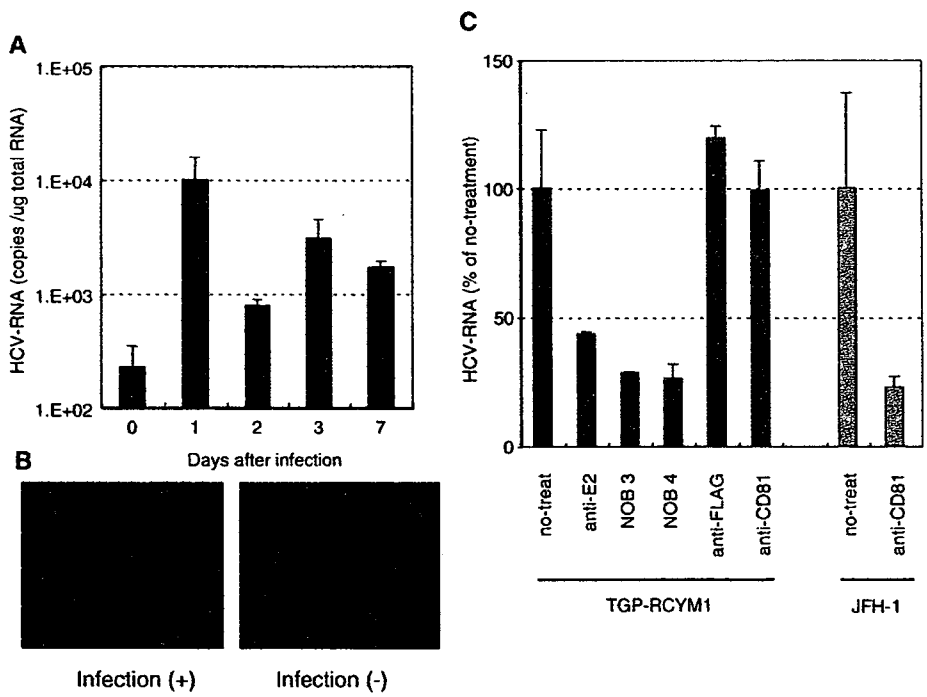

Fig. 6. Infectivity of HCV-LPs secreted from TGP-cultured RCYM1 cells and neutralization of the infection. (A) Kinetics of HCV RNA after the infection of HCV-LPs. Huh-7.5.1 cells were infected with HCV-LPs and harvested at days 0, 1, 2, 3, and 7. HCV RNAs in the cells were determined by real-time RT-PCR. (B) Huh-7.5.1 cells infected with HCV-LPs (upper panel) or without infection (lower panel) were cultured for 4 days, followed by immunostaining with anti-NS5A antibody. Nuclei were counterstained with 4′,6-diamidino-2-phenylindole (DAPI). (C) Huh-7.5.1 cells were infected with HCV-LPs after pretreatment with anti-E2 antibody AP33, neutralization of binding (NOB) antibodies, or anti-FLAG antibody. Anti-human CD81 antibody was preincubated with Huh-7.5.1 cells prior to the infection. Huh-7.5.1 cells were infected with HCV-LPs derived from TGP-cultured RCYM1cells or JFH1 virus and incubated for 4 days; HCV RNAs in the cells were determined by real-time RT-PCR. The inhibition rate is given as the percentage of the no-treatment controls. Average values with standard deviations in triplicate samples are shown. Closed bars, HCV-LPs secreted from TGP-cultured RCYM1 cells; shaded bars, JFH1 virus.

and 26% in the presence of AP33, NOB3, and NOB4, respectively. No reduction of viral RNA in infected cells was observed following treatment with anti-FLAG antibody. Thus, the present results suggest that viral envelope proteins play a crucial role in the infectivity of HCV-LPs produced by RCYM1 cells cultured in TGP. We further tested anti-CD81 antibody for inhibition of the virus infection in our system. As shown in Fig. 6C, pretreatment of the cells with the anti-CD81 antibody resulted in no inhibition of the intracellular HCV RNA level in the infected cells. In contrast, under the same condition of treatment, the antibody efficiently inhibited the infection of JFH-1 virus, which was produced from the HCV JFH-1 molecular clone as previously described (Wakita et al., 2005; Zhong et al., 2005), suggesting that CD81 has no or little, if any, need for the infection of HCV produced in our system.

Potential use of the TGP culture system for HCV production and evaluation of antiviral agents

In a recent report, Lindenbach et al. (2005) found that a cell culture system supporting complete replication of an HCV genotype 2a clone is useful for the evaluation of antiviral drugs. However, to date this complete HCV culture system has not been extended to genotype 1b, which is more frequently detected in patients with hepatitis C and is the most difficult to treat.

We show here the potential utility of the TGP culture of RCYM1 cells for evaluating anti-HCV drugs (Fig. 7). Intracellular HCV RNA levels in TGP-cultured RCYM1 cell spheroids were reduced by 90% after 3 days of culture with 100 IU/ml of IFN-α (Fig. 7A). Likewise, the extracellular HCV particle level, which was calculated using the HCV RNA copy number of the 1.18 g/ml supernatant fraction, was reduced by 89% by IFN-α treatment (Fig. 7B). Moreover, the production of HCV particles was inhibited by treatment with 100 μM RBV to the same degree (85%) as intracellular HCV RNA (Fig. 7B). The level of HCV RNA detected in the 1.04 g/ml fraction of the culture supernatant of the untreated group was approximately one fourteenth of that in the 1.18 g/ml fraction, and the level increased with the addition of IFN-α or RBV (Fig. 7B). Although the mechanism underlying this increase is unknown, a similar phenomenon was observed when several highly cytotoxic agents were evaluated using TGP-RCYM1 cultures (data not shown). It is therefore likely that some cellular proteins associated with HCV RNA are released into the culture supernatant as a result of cell death caused by the moderate cytotoxic effects of IFN and RBV.

Collectively, these results demonstrate that the HCV production model based on TGP culture is useful for evaluating HCV particle production and the inhibitory effects of anti-HCV drugs.

Discussion

In the present report, we describe that HCV-LPs are assembled and released from Huh-7 cells harboring a dicistronic genome-length Con1 HCV RNA in two independent 3D culture systems. The HCV-LPs closely resemble virus-like particles detected in the sera of patients with hepatitis C in terms of both particle size and morphology. The HCV-LPs released into the culture supernatant have a buoyant density of approximately 1.18 g/ml, which is much higher than that of putative HCV particles isolated from patient sera reported previously (Andre et al., 2002; Kanto et al., 1994; Nakajima et al., 1996; Trestard et al., 1998) and slightly higher than the average density of virus particles produced with the JFH-1 isolate (Wakita et al., 2005). One possible explanation is that the HCV particles are highly bound to lipids and low-density lipoproteins in patient sera. In agreement with a recent report (Wakita et al., 2005), our EM examination demonstrated that HCV-LPs are 50–60 nm in diameter and are composed of core-like particles with a diameter of approximately 30 nm that are surrounded by ER-derived E1/

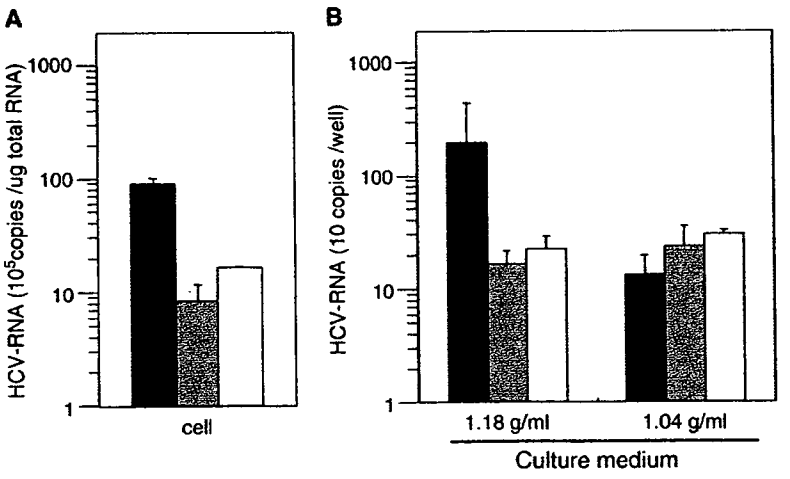

Fig. 7. Inhibition of HCV-LP production by IFN and RBV. TGP-cultured RCYM1 cells were treated with 100 IU/ml IFN-α or 100 μM RBV, and HCV RNAs in the cells (A) and in the culture media (B) were then determined. Culture media from each sample were fractionated by sucrose gradient centrifugation and HCV-LP positive (1.18 g/ml) and negative (1.04 g/ml) fractions were assayed. Average values with standard deviations in triplicate samples are shown. Closed bars, no-treatment control; shaded bars, IFN-α; open bars, RBV.

E2 proteins. These particles are observed at the ER membranes and in dilated cisternae of the ER, suggesting that the interaction of the ER membrane containing HCV envelope proteins with the viral core protein drives the budding process of HCV particles into the ER lumen.

Although studies on the ultrastructure and morphogenesis of HCV-LPs have been conducted using recombinant viral vectors carrying HCV structural protein genes (Baumert et al., 1998; Blanchard et al., 2002, 2003), the present study provides the first visual evidence of assembly and budding of HCV particles in a heterologous expression system in which a full-length viral genome is replicating and the viral particles are secreted into the culture medium. We also demonstrated that the HCV-LPs produced in our 3D culture system are infectious and that their infection is prevented by the monoclonal antibody AP33 directed against E2 (Owsianka et al., 2005) as well as by NOB antibodies (Ishii et al., 1998), which are sera of patients naturally resolving from chronic hepatitis C and exhibiting neutralizing activity. This result is consistent with the recent demonstration that E2 is required for the infectivity of JFH-1 virus (Wakita et al., 2005). It has been shown that CD81 interacts with E2 (Pileri et al., 1998) and that anti-CD81 antibodies or a soluble CD81 fragment block the infection of Huh-7 cells with either pseudotyped retroviral particles, JFH-1 virus or J6/JFH1 chimera (Lindenbach et al., 2005; Netski et al., 2005; Wakita et al., 2005; Zhong et al., 2005). Inconsistent with these studies, however, we found that anti-CD81 antibody did not inhibit the virus infection in our system. Although CD81 is considered to represent an important component in HCV entry, there are several other candidate cellular receptors for HCV (Bartosch and Cosset, 2006) and a study has demonstrated that in vitro binding of HCV to hepatoma cell lines was not inhibited by the anti-CD81 antibody (Sasaki et al., 2003).

In a previous report (Aizaki et al., 2003), we describe the production and release of infectious HCV particles from a human hepatocellular carcinoma-derived cell line, FLC4, using RFB culture in two experiments: inoculation of cells with infectious plasma from an HCV carrier and transfection of cells with viral RNA transcribed from the full-length cDNA of genotype 1a, which is known to infect chimpanzees. These findings prompted us to use the RFB system to create a culture model of HCV production based on genome-length dicistronic viral RNA, which has not been found to produce viral particles in standard monolayer cultures. As expected, HCV-LPs were produced and secreted into the medium during RFB culture of RCYM1 cells, whereas virus production was not observed in the conventional monolayer culture of RCYM1 cells. The presence of the viral envelope protein(s) on the HCV-LPs obtained in the RFB culture was strongly suggested from their density analysis with and without NP40 treatment.

We also created another 3D environment supportive of RCYM1 culture using TGP, a chemically synthesized biocompatible polymer which has a sol-gel transition temperature, thus enabling us to culture cells three-dimensionally in the gel phase at 37 °C and to harvest them in the sol phase at 4 °C, without enzyme digestion (Yoshioka et al., 1994). In contrast to other matrix gels made from conventional natural polymers and developed for 3D culture, including matrigel (Kleinman et al., 1986), collagen gel (Lawler et al., 1983), and soft agar, TGP has several advantages that allow us to investigate the functional characteristics of epithelial cells, their tissue-like morphology, and their potential clinical applications. The use of 3D culture materials other than TGP requires treatment with appropriate digestive enzymes or heating to collect cells grown as spheroids from the culture media, and the matrices may damage the cultured cells to some extent. Thus, it is difficult to keep the viable cells in a functionally and structurally intact. In addition, because matrigel and collagen gel are made from animal or tumor tissue, the possibility that certain pathogens or unidentified factors might influence cell function cannot be excluded. In the present study, we found that Huh-7 and RCYM1 cells formed an organized structure of spheroids after 7–10 days of culture in TGP, and that HCV-LPs were assembled and released from RCYM1 spheroids, as observed in RFB culture. It can be ruled out that HCV-LPs, RNA, and core protein detected in the TGP culture supernatant are released by damaged and/or broken cells because neither digestive enzymes nor heating is used in the culture procedures and no cell damage has been observed in the cultures.

It remains to be clarified why HCV particles were produced from Huh-7 cells harboring the genome-length dicistronic HCV RNA more efficiently in the 3D cultures than in the monolayer cultures. However, this might be related to the fact that directional protein transport in hepatocytes occurs more readily in 3D culture. EM examination demonstrated that, in the RFB and TGP culture systems, human hepatoma cells, such as Huh-7, FLC4, and FLC5 cells, self-assemble into spheroids with possible polarized morphology in which microvilli develop on the cell surface and channels resembling bile canaliculi and junction structures are created in the intercellular spaces (Aizaki et al., 2003; Iwahori et al., 2003). In contrast, human hepatoma cells adhere when grown on a plastic surface, growing as a flat monolayer without exhibiting the characteristics of polarized epithelium. In general, the interaction of viruses with polarized epithelia in the host is one of the key steps in the viral life cycle. A variety of viruses, especially enveloped viruses, mature and bud from distinct membrane domains of the host cells (Compans, 1995; Garoff et al., 1998; Schmitt and Lamb, 2004; Takimoto and Portner, 2004). For example, several respiratory viruses, such as influenza virus, parainfluenza virus, rhinovirus, and respiratory syncytial virus, are released preferentially from the apical surface. Conversely, other viruses egress from the basolateral membrane; these include vesicular stomatitis virus, Semliki Forest virus, vaccinia virus, and certain retroviruses. Thus, it is likely that more organized intracellular trafficking pathways exist in the 3D culture of Huh-7-derived cells, thereby driving the assembly and release of HCV.

The efficient production of HCV in 3D cultures could also be due to the reduction of HCV RNA replication and/or translation in 3D cultures as compared to those in monolayer cultures. RNA replication and/or translation of HCV replicons in Huh-7 cells are highly dependent on host cell growth (Pietschmann et al., 2001). In the present study, we found that the slow growth of spheroids resulted in reduced expression of HCV protein and

viral RNA in 3D-cultured RCYM1 cells compared to that in monolayer cultures containing similar cell numbers. The doubling time of cells grown in TGP or RFB culture was approximately twice that observed in monolayer culture. Although it is possible that amino acid substitutions of culture-adaptive mutations contribute to interference with virus production, another possibility might be that in cases of certain HCV clones, higher expression of the viral proteins leads to their misfolding, thereby precluding the formation of virus particles.

Complete cell culture systems for HCV have recently been developed (Lindenbach et al., 2005; Wakita et al., 2005; Zhong et al., 2005) using a genotype 2a isolate, JFH-1, obtained from a Japanese patient with fulminant hepatitis (Date et al., 2004; Kato et al., 2001, 2003). Unlike many other HCV isolates, JFH-1-based subgenomic replicons do not require culture-adaptive mutations for efficient RNA replication (Kato et al., 2003). Transfection of Huh-7 cells with the full-length JFH-1 genome or a chimeric genome using JFH-1 and J6 results in the efficient production of infectious HCV (Lindenbach et al., 2005; Wakita et al., 2005; Zhong et al., 2005). This newly established HCV culture system is undoubtedly useful for a variety of HCV studies; however, these systems rely on the JFH-1 replicase (NS3 to 5B) and little is known about the reasons that this particular isolate permits efficient HCV production. Virus yield in the 3D systems presented here is significantly lower than that in systems based on JFH-1; it seems that 0.1–1 copies of HCV RNA/cell/day are generated and assembled into viral particles. The ratio of viral RNA to the core protein in these fractions is approximately 10^5 RNA copies/1 fmol of the core. Although only moderate production of HCV particles is observed in 3D culture of RCYM1 cells, this is the first study to demonstrate the production of infectious HCV particles derived from genotype 1b, which is highly prevalent worldwide and is thought to present a higher risk of developing hepatocellular carcinoma and/or cirrhosis than infections with other HCV types (Bruno et al., 1997; Silini et al., 1996). The findings of the present study may also suggest that an extremely high efficiency of viral replication, such as that observed in the case of JFH-1 isolate, is not needed to produce HCV particles in 3D cultures of Huh-7 cells. Heller et al. (2005) report HCV virion production in a culture transfected with the genomic cDNA of genotype 1b; however, the infectivity of the virus particles remains to be determined. More recently, it was shown that chimeric HCV containing structural proteins of genotypes 1a, 1b, or 3a was produced from fusion of the core to the p7 or NS2 region with downstream nonstructural regions of JFH1 clone, but that intergenotypic chimeras frequently yielded lower titers of infectious HCV compared to JFH1 or J6/JFH1 chimera (Pietschmann et al., personal communication). The 3D culture system described in the present study might be a helpful method of increasing the efficiency of assembly and release of intergenotypic chimeric HCV.

In summary, we found that the expression of dicistronic genome-length Con1 HCV RNA of genotype 1b in 3D-cultured Huh-7 cells yields infectious virus particles, and we demonstrated the usefulness for producing HCV particles of two 3D culture systems based on RFB and TGP, in which human hepatoma cells can assemble into spheroids with potentially polarized morphology. HCV morphogenesis occurs in a complex cellular environment in which host factors may either enhance or reduce the assembly and budding process. The culture system described here will allow us to further study viral morphogenesis and the biophysical properties of HCV particles, and it provides a new tool for the future development of anti-HCV drugs.

Materials and methods

Cell lines bearing dicistronic HCV RNAs

To generate a stable cell line harboring genome-length dicistronic HCV RNA, we electroporated 10^7 Huh-7 cells with 50 μg of the RNA transcribed from a plasmid pFKI389neo/core-3′/NK5.1 (Pietschmann et al., 2002). The cells were maintained in Dulbecco's modified Eagle's medium with 10% fetal bovine serum and 0.5 mg/ml G418 (Promega). After stringent selection for 3 weeks, a fast-growing clone was isolated and designated as RCYM1. A Huh-7-derived cell line, 5–15, harboring a subgenomic replicon (Lohmann et al., 1999) was also used.

3D cell cultures

The RFB system (Able, Japan) was manipulated as described previously (Aizaki et al., 2003) with minor modifications. Briefly, the RFB column, being filled with 4 ml of porous carrier beads made from polyvinyl alcohol, seeded with 1×10^7 of RCYM1 or 5–15 cells. The cells were cultured in ASF104 medium (Ajinomoto, Japan) supplemented with 4 g/l of D-glucose, 2% fetal calf serum, and 0.5 mg/ml of G418 (Promega). TGP (Mebiol Gel MB-10; Mebiol, Japan) was supplied as a lyophilized form and its aqueous solution was prepared before use as previously described (Hishikawa et al., 2004; Nagaya et al., 2004; Yoshioka et al., 1994). Briefly, TGP in a flask was dissolved in 10 ml of the culture medium and was maintained at 4 °C overnight. To prepare HCV particles, we suspended 5×10^6 cells of RCYM1 in 10 ml of TGP solution and aliquots were poured into a multi-well plate. Upon warming to 37 °C, the TGP solution quickly turned into a gel form, and 3 volumes of the culture medium were added to cover the gel. To recover spheroid cells and the culture supernatant after cultivation, we subjected the cultured plate to a temperature of 4 °C for 10 min to dissolve the gel. In order to separate spheroid cells from the culture medium, we subsequently centrifuged the TGP culture diluted with the overlaid culture medium at 1000×*g* for 5 min.

Sucrose density gradient centrifugation

The culture medium collected from the RFB or TGP was centrifuged at 8000 × *g* for 50 min to remove all cellular debris, after which the supernatant was centrifuged at 25,000 rpm at 4 °C for 4 h with an SW28 rotor (Beckman). The precipitant was suspended in 1 ml of TNE buffer [10 mM Tris–HCl (pH 7.8), 1 mM EDTA, 100 mM NaCl] and was then layered on top of continuous 10–60% (wt/vol) sucrose gradient in TNE buffer,

followed by centrifugation at 35,000 rpm at 4 °C for 14 h with an SW41E rotor (Beckman). Fractions (1 ml each) were collected from the top of the tube (12 fractions in total). The density of each fraction was determined by the weight of 100 μl of the fraction. For NP40 treatment, 0.5 ml of the TNE-suspended sample as described above was supplemented with 10 μl of RNase inhibitor (Takara, Japan) and 5 μl of 1M DTT, which was diluted by adding NP40 solution to a final concentration of 0.2%. After incubation at 4 °C for 20 min, the sample was fractionated by discontinuous 10–60% sucrose gradient centrifugation.

Quantitation of HCV RNA and core protein

Total RNA was extracted from cells and from the culture medium using TRIZOL (Invitrogen) and a QIAamp Viral RNA Mini spin column (Qiagen), respectively. Real-time RT-PCR was performed using TaqMan EZ RT-PCR Core Reagents (PE Applied Biosystems), as described previously (Aizaki et al., 2004; Suzuki et al., 2005). HCV core antigen within cells and culture medium was measured by immunoassay (Ortho HCV-Core ELISA Kit; Ortho-Clinical Diagnotics), following the manufacturer's instructions.

Western blot analysis

The protein concentration of cells recovered from monolayer or 3D cultures was determined by BCA Protein Assay Kit (Pierce). Aliquots of samples were analyzed by sodium dodecyl sulfate–polyacrylamide gel electrophoresis (SDS–PAGE) and transferred to polyvinylidene difluoride membranes (Immobilon; Millipore, Japan) using a semidry blotter. After overnight incubation at 4 °C in blocking buffer (Dainippon Pharmaceuticals, Japan) with 0.2% Tween 20, the membranes were incubated with appropriately diluted anti-HCV core (Anogen) and anti-NS5A (Austral Biologicals) monoclonal antibody, followed by incubation with horseradish peroxidase conjugated anti-mouse immunoglobulin G (Cell Signaling). The blots were then washed and developed with enhanced SuperSignal West Pico Chemiluminecent Substrate (Pierce).

Immunocytochemistry

For NS5A staining, infected cells cultured on collagen-coated coverslips were washed with phosphate buffered saline (PBS) and fixed with 4% paraformaldehyde at 4 °C for 30 min, followed by permeabilization with PBS containing 0.2% TritonX-100. After preincubation with BlockAce (Dainippon Pharmaceuticals), the samples were stained using mouse anti-NS5A antibody and rhodamine-conjugated goat anti-mouse IgG (ICN Pharmaceuticals) as the first and second antibodies, respectively.

Electron microscopy

To visualize HCV-LPs secreted into the medium, we concentrated and adsorbed sucrose density fractions prepared as described above onto carbon-coated grids for 1 min. The grids were stained with 1% uranyl acetate for 1 min and examined under a Hitachi H-7600 transmission electron microscope. To prepare thin sections of HCV-LPs, we prefixed precipitated HCV-LPs in 2% glutaraldehyde–0.1 M cacodylate buffer at 4 °C overnight, followed by three rounds of washing with 0.1 M cacodylate buffer. The samples were then postfixed in 2% osmium tetroxide at 4 °C for 2 h, dehydrated in a graded series of ethanol solutions followed by propylene oxide, and embedded in a mixture of EPON 812, dodecenyl succinic anhydride (DDSA), methyl nadic anhydrate (MNA), and 2,4,6-tri (dimethylaminomethyl) phenol (DMP-30) at 60 °C for 2 days. Thin sections (80 nm) were stained with uranyl acetate and lead citrate. For electron microscopy of RCYM1 cells cultured in TGP, the cells were prefixed in 2% glutaraldehyde–0.1 M cacodylate buffer at 4 °C for 1 h and washed three times with 0.1 M cacodylate buffer, followed by postfixation in 2% osmium tetroxide for 3 h. After dehydration in a graded series of ethanol solutions and propylene oxide, the cells were embedded in a mixture of Epoxy 812, DDSA, MNA, and DMP-30 at 60 °C for 2 days. Thin sections (60–80 nm) were stained with 2% uranyl acetate.

Immunoelectron microscopy

HCV-LP samples were adsorbed on formvar-carbon grids and then floated for 30 min on a drop of BlockAce. Diluted anti-E2 mouse antibody was then applied for 1 h. After three rounds of washing, diluted anti-mouse IgG conjugated with 5-nm gold particles was applied for 1 h, and the grids were then stained with 1% uranyl acetate. In order to perform immunoelectron microscopy of TGP cultures using silver-intensified immunogold labeling, we fixed the cells in 4% paraformaldehyde–0.1% glutaraldehyde with 0.15 M HEPES buffer at 4 °C, followed by incubation with either anti-core rabbit antibody or anti-E1 mouse antibody overnight. After several washings, anti-rabbit or anti-mouse secondary antibody coupled with 1.4-nm-diameter gold particles (Nanoprobes) was applied overnight. The samples were then washed and fixed in 2% glutaraldehyde in 0.1 M sodium cacodylate buffer (pH 7.4) for 3 h, followed by enlargement of the gold particles with an HQ-Silver Enhancement Kit (Nanoprobes). For double staining with anti-E1 and anti-core antibodies, the cells were fixed in 7% paraformaldehyde–0.25 M sucrose in 0.03% picric acid–0.05 M cacodylate buffer at pH 7.4. Ten-nanometer gold particle-coupled anti-rabbit and 5-nm gold particle-coupled anti-mouse antibodies were used as secondary antibodies.

Assays for the infectivity of HCV-LPs and neutralization of the infection

Cell supernatant from 3D-cultured RCYM1 cells was centrifuged at 8000 × *g* for 50 min to remove all cellular debris, after which the supernatant was centrifuged at 25,000 rpm at 4 °C for 4 h with an SW28 rotor. The precipitant was suspended in 0.2–0.5 ml of ASF104 medium and the aliquot containing approximately 1×10^5 HCV RNA copies was used as each inoculum. Huh-7.5.1

cells (provided by Dr. F. V. Chisari, The Scripps Research Institute) (Zhong et al., 2005), which were seeded at a density of 10^4 cells/well in a 48-well plate 24 h before infection. The inocula were incubated for 3 h, followed by 3 rounds of washing with PBS and the addition of complete medium. For the kinetics assay, cells were harvested 0, 1, 2, 3, and 7 days after infection and the amount of intracellular HCV RNA was quantified as described above. Infection with HCV-LP was determined after 4 days by immunofluorescence staining for HCV NS5A. In the neutralization assay, the HCV-LP samples were incubated with the anti-E2 antibody AP33 (Owsianka et al., 2005) at 10 μg/ml (kindly provided by Dr. A. H. Patel, University of Glasgow, UK), with the human sera with high titers of NOB antibodies NOB3 and NOB4 (Ishii et al., 1998), or with anti-FLAG antibody (Sigma) at 10 μg/ml for 1 h at 37 °C prior to infection. Anti-human CD81 antibody (BD Pharmigen) at 10 μg/ml was preincubated with Huh-7.5.1 cells for 1 h at 37 °C, followed by being washed with PBS three times. HCV-LP derived from TGP-cultured RCYM1 cells or JFH1 virus was incubated with these cells, as mentioned above. JFH1 virus was prepared from pJFH1 (Wakita et al., 2005), which contains the full-length cDNA of JFH1 isolate and was kindly provided by T. Wakita (Tokyo Metropolitan Institute for Neuroscience, Japan), as described (Wakita et al., 2005). The cells were harvested 4 days after infection and neutralizing activity was assessed by quantifying the amount of intracellular HCV RNA as described above.

Assay for anti-HCV-LP production

At the initiation of the 3D culture of RCYM1 cells (5×10^5 in 1 ml TGP), 100 IU/ml IFN-α (Sumiferon 300; Sumitomo Pharmaceuticals, Japan), or 100 μM RBV (MP Biomedicals, Germany) were added and the cells were cultured for 5 days. Culture media were harvested and fractionated by sucrose density centrifugation as described above. Total RNAs were extracted from aliquots of 1.18 g/ml (HCV-LP positive) and 1.04 g/ml (HCV-LP-negative) fractions, followed by quantification of viral RNA.

Acknowledgments

The authors would like to thank Francis V. Chisari of The Scripps Research Institute, Arvind H. Patel of the University of Glasgow, and Takaji Wakita of Tokyo Metropolitan Institute for Neuroscience for providing Huh-7.5.1 cells, anti-E2 antibody, and pJFH1, respectively. We also thank Mami Matsuda, Tetsu Shimoji, and Makiko Yahata for technical assistance, and Tomoko Mizoguchi for her secretarial work. This work was supported in part by a grant for Research on Health Sciences focusing on Drug Innovation from the Japan Health Sciences Foundation; by grants-in-aid from the Ministry of Health, Labor and Welfare; by a Sasagawa Scientific Research Grant from the Japan Science Society; and by the program for Promotion of Fundamental Studies in Health Sciences of the National Institute of Biomedical Innovation (NBIO), Japan; and by the New Energy and Industrial Technology Development Organization (NEDO) of Japan.

References

Aizaki, H., Nagamori, S., Matsuda, M., Kawakami, H., Hashimoto, O., Ishiko, H., Kawada, M., Matsuura, T., Hasumura, S., Matsuura, Y., Suzuki, T., Miyamura, T., 2003. Production and release of infectious hepatitis C virus from human liver cell cultures in the three-dimensional radial-flow bioreactor. Virology 314, 16–25.

Aizaki, H., Lee, K.J., Sung, V.M., Ishiko, H., Lai, M.M., 2004. Characterization of the hepatitis C virus RNA replication complex associated with lipid rafts. Virology 324, 450–461.

Andre, P., Komurian-Pradel, F., Deforges, S., Perret, M., Berland, J.L., Sodoyer, M., Pol, S., Brechot, C., Paranhos-Baccala, G., Lotteau, V., 2002. Characterization of low- and very-low-density hepatitis C virus RNA-containing particles. J. Virol. 76, 6919–6928.

Bartosch, B., Cosset, F.L., 2006. Cell entry of hepatitis C virus. Virology (Electronic publication ahead of print).

Baumert, T.F., Ito, S., Wong, D.T., Liang, T.J., 1998. Hepatitis C virus structural proteins assemble into viruslike particles in insect cells. J. Virol. 72, 3827–3836.

Blanchard, E., Brand, D., Trassard, S., Goudeau, A., Roingeard, P., 2002. Hepatitis C virus-like particle morphogenesis. J. Virol. 76, 4073–4079.

Blanchard, E., Hourioux, C., Brand, D., Ait-Goughoulte, M., Moreau, A., Trassard, S., Sizaret, P.Y., Dubois, F., Roingeard, P., 2003. Hepatitis C virus-like particle budding: role of the core protein and importance of its Asp111. J. Virol. 77, 10131–10138.

Blight, K.J., Kolykhalov, A.A., Rice, C.M., 2000. Efficient initiation of HCV RNA replication in cell culture. Science 290, 1972–1974.

Blight, K.J., McKeating, J.A., Rice, C.M., 2002. Highly permissive cell lines for subgenomic and genomic hepatitis C virus RNA replication. J. Virol. 76, 13001–13014.

Bruno, S., Silini, E., Crosignani, A., Borzio, F., Leandro, G., Bono, F., Asti, M., Rossi, S., Larghi, A., Cerino, A., Podda, M., Mondelli, M.U., 1997. Hepatitis C virus genotypes and risk of hepatocellular carcinoma in cirrhosis: a prospective study. Hepatology 25, 754–758.

Choo, Q.L., Kuo, G., Weiner, A.J., Overby, L.R., Bradley, D.W., Houghton, M., 1989. Isolation of a cDNA clone derived from a blood-borne non-A, non-B viral hepatitis genome. Science 244, 359–362.

Choo, Q.L., Richman, K.H., Han, J.H., Berger, K., Lee, C., Dong, C., Gallegos, C., Coit, D., Medina-Selby, R., Barr, P.J., et al., 1991. Genetic organization and diversity of the hepatitis C virus. Proc. Natl. Acad. Sci. U.S.A. 88, 2451–2455.

Compans, R.W., 1995. Virus entry and release in polarized epithelial cells. Curr. Top. Microbiol. Immunol. 202, 209–219.

Date, T., Kato, T., Miyamoto, M., Zhao, Z., Yasui, K., Mizokami, M., Wakita, T., 2004. Genotype 2a hepatitis C virus subgenomic replicon can replicate in HepG2 and IMY-N9 cells. J. Biol. Chem. 279, 22371–22376.

Davis, G.L., Wong, J.B., McHutchison, J.G., Manns, M.P., Harvey, J., Albrecht, J., 2003. Early virologic response to treatment with peginterferon alfa-2b plus ribavirin in patients with chronic hepatitis C. Hepatology 38, 645–652.

Frese, M., Pietschmann, T., Moradpour, D., Haller, O., Bartenschlager, R., 2001. Interferon-alpha inhibits hepatitis C virus subgenomic RNA replication by an MxA-independent pathway. J. Gen. Virol. 82, 723–733.

Garoff, H., Hewson, R., Opstelten, D.J., 1998. Virus maturation by budding. Microbiol. Mol. Biol. Rev. 62, 1171–1190.

Grakoui, A., McCourt, D.W., Wychowski, C., Feinstone, S.M., Rice, C.M., 1993. Characterization of the hepatitis C virus-encoded serine proteinase: determination of proteinase-dependent polyprotein cleavage sites. J. Virol. 67, 2832–2843.

Guo, J.T., Bichko, V.V., Seeger, C., 2001. Effect of alpha interferon on the hepatitis C virus replicon. J. Virol. 75, 8516–8523.

Heller, T., Saito, S., Auerbach, J., Williams, T., Moreen, T.R., Jazwinski, A., Cruz, B., Jeurkar, N., Sapp, R., Luo, G., Liang, T.J., 2005. An in vitro model of hepatitis C virion production. Proc. Natl. Acad. Sci. U.S.A. 102, 2579–2583.

Hijikata, M., Kato, N., Ootsuyama, Y., Nakagawa, M., Shimotohno, K., 1991. Gene mapping of the putative structural region of the hepatitis C virus genome by in vitro processing analysis. Proc. Natl. Acad. Sci. U.S.A. 88, 5547–5551.

Hishikawa, K., Miura, S., Marumo, T., Yoshioka, H., Mori, Y., Takato, T., Fujita, T., 2004. Gene expression profile of human mesenchymal stem cells during osteogenesis in three-dimensional thermoreversible gelation polymer. Biochem. Biophys. Res. Commun. 317, 1103–1107.

Ikeda, M., Yi, M., Li, K., Lemon, S.M., 2002. Selectable subgenomic and genome-length dicistronic RNAs derived from an infectious molecular clone of the HCV-N strain of hepatitis C virus replicate efficiently in cultured Huh7 cells. J. Virol. 76, 2997–3006.

Ishii, K., Rosa, D., Watanabe, Y., Katayama, T., Harada, H., Wyatt, C., Kiyosawa, K., Aizaki, H., Matsuura, Y., Houghton, M., Abrignani, S., Miyamura, T., 1998. High titers of antibodies inhibiting the binding of envelope to human cells correlate with natural resolution of chronic hepatitis C. Hepatology 28, 1117–1120.

Iwahori, T., Matsuura, T., Maehashi, H., Sugo, K., Saito, M., Hosokawa, M., Chiba, K., Masaki, T., Aizaki, H., Ohkawa, K., Suzuki, T., 2003. CYP3A4 inducible model for in vitro analysis of human drug metabolism using a bioartificial liver. Hepatology 37, 665–673.

Kanto, T., Hayashi, N., Takehara, T., Hagiwara, H., Mita, E., Naito, M., Kasahara, A., Fusamoto, H., Kamada, T., 1994. Buoyant density of hepatitis C virus recovered from infected hosts: two different features in sucrose equilibrium density-gradient centrifugation related to degree of liver inflammation. Hepatology 19, 296–302.

Kato, T., Furusaka, A., Miyamoto, M., Date, T., Yasui, K., Hiramoto, J., Nagayama, K., Tanaka, T., Wakita, T., 2001. Sequence analysis of hepatitis C virus isolated from a fulminant hepatitis patient. J. Med. Virol. 64, 334–339.

Kato, T., Date, T., Miyamoto, M., Furusaka, A., Tokushige, K., Mizokami, M., Wakita, T., 2003. Efficient replication of the genotype 2a hepatitis C virus subgenomic replicon. Gastroenterology 125, 1808–1817.

Kawada, M., Nagamori, S., Aizaki, H., Fukaya, K., Niiya, M., Matsuura, T., Sujino, H., Hasumura, S., Yashida, H., Mizutani, S., Ikenaga, H., 1998. Massive culture of human liver cancer cells in a newly developed radial flow bioreactor system: ultrafine structure of functionally enhanced hepatocarcinoma cell lines. In Vitro Cell. Dev. Biol. Anim. 34, 109–115.

Kleinman, H.K., McGarvey, M.L., Hassell, J.R., Star, V.L., Cannon, F.B., Laurie, G.W., Martin, G.R., 1986. Basement membrane complexes with biological activity. Biochemistry 25, 312–318.

Lawler, E.M., Miller, F.R., Heppner, G.H., 1983. Significance of three-dimensional growth patterns of mammary tissues in collagen gels. In Vitro 19, 600–610.

Lindenbach, B.D., Evans, M.J., Syder, A.J., Wolk, B., Tellinghuisen, T.L., Liu, C.C., Maruyama, T., Hynes, R.O., Burton, D.R., McKeating, J.A., Rice, C.M., 2005. Complete replication of hepatitis C virus in cell culture. Science 309, 623–626.

Lohmann, V., Korner, F., Koch, J., Herian, U., Theilmann, L., Bartenschlager, R., 1999. Replication of subgenomic hepatitis C virus RNAs in a hepatoma cell line. Science 285, 110–113.

Manns, M.P., McHutchison, J.G., Gordon, S.C., Rustgi, V.K., Shiffman, M., Reindollar, R., Goodman, Z.D., Koury, K., Ling, M., Albrecht, J.K., 2001. Peginterferon alfa-2b plus ribavirin compared with interferon alfa-2b plus ribavirin for initial treatment of chronic hepatitis C: a randomised trial. Lancet 358, 958–965.

Matsuura, T., Kawada, M., Hasumura, S., Nagamori, S., Obata, T., Yamaguchi, M., Hataba, Y., Tanaka, H., Shimizu, H., Unemura, Y., Nonaka, K., Iwaki, T., Kojima, S., Aizaki, H., Mizutani, S., Ikenaga, H., 1998. High density culture of immortalized liver endothelial cells in the radial-flow bioreactor in the development of an artificial liver. Int. J. Artif. Organs 21, 229–234.

Nagaya, M., Kubota, S., Suzuki, N., Tadokoro, M., Akashi, K., 2004. Evaluation of thermoreversible gelation polymer for regeneration of focal liver injury. Eur. Surg. Res. 36, 95–103.

Nakajima, N., Hijikata, M., Yoshikura, H., Shimizu, Y.K., 1996. Characterization of long-term cultures of hepatitis C virus. J. Virol. 70, 3325–3329.

Netski, D.M., Mosbruger, T., Depla, E., Maertens, G., Ray, S.C., Hamilton, R.G., Roundtree, S., Thomas, D.L., McKeating, J., Cox, A., 2005. Humoral immune response in acute hepatitis C virus infection. Clin. Infect. Dis. 41, 667–675.

Owsianka, A., Tarr, A.W., Juttla, V.S., Lavillette, D., Bartosch, B., Cosset, F.L., Ball, J.K., Patel, A.H., 2005. Monoclonal antibody AP33 defines a broadly neutralizing epitope on the hepatitis C virus E2 envelope glycoprotein. J. Virol. 79, 11095–11104.

Pietschmann, T., Lohmann, V., Rutter, G., Kurpanek, K., Bartenschlager, R., 2001. Characterization of cell lines carrying self-replicating hepatitis C virus RNAs. J. Virol. 75, 1252–1264.

Pietschmann, T., Lohmann, V., Kaul, A., Krieger, N., Rinck, G., Rutter, G., Strand, D., Bartenschlager, R., 2002. Persistent and transient replication of full-length hepatitis C virus genomes in cell culture. J. Virol. 76, 4008–4021.

Pileri, P., Uematsu, Y., Campagnoli, S., Galli, G., Falugi, F., Petracca, R., Weiner, A.J., Houghton, M., Rosa, D., Grandi, G., Abrignani, S., 1998. Binding of hepatitis C virus to CD81. Science 282, 938–941.

Rosa, D., Campagnoli, S., Moretto, C., Guenzi, E., Cousens, L., Chin, M., Dong, C., Weiner, A.J., Lau, J.Y., Choo, Q.L., Chien, D., Pileri, P., Houghton, M., Abrignani, S., 1996. A quantitative test to estimate neutralizing antibodies to the hepatitis C virus: cytofluorimetric assessment of envelope glycoprotein 2 binding to target cells. Proc. Natl. Acad. Sci. U.S.A. 93, 1759–1763.

Sasaki, M., Yamauchi, K., Nakanishi, T., Kamogawa, Y., Hayashi, N., 2003. In vitro binding of hepatitis C virus to CD81-positive and -negative human cell lines. J. Gastroenterol. Hepatol. 18, 74–79.

Schmitt, A.P., Lamb, R.A., 2004. Escaping from the cell: assembly and budding of negative-strand RNA viruses. Curr. Top. Microbiol. Immunol. 283, 145–196.

Shimizu, Y.K., Feinstone, S.M., Kohara, M., Purcell, R.H., Yoshikura, H., 1996. Hepatitis C virus: detection of intracellular virus particles by electron microscopy. Hepatology 23, 205–209.

Silini, E., Bottelli, R., Asti, M., Bruno, S., Candusso, M.E., Brambilla, S., Bono, F., Iamoni, G., Tinelli, C., Mondelli, M.U., Ideo, G., 1996. Hepatitis C virus genotypes and risk of hepatocellular carcinoma in cirrhosis: a case–control study. Gastroenterology 111, 199–205.

Suzuki, T., Omata, K., Satoh, T., Miyasaka, T., Arai, C., Maeda, M., Matsuno, T., Miyamura, T., 2005. Quantitative detection of hepatitis C virus (HCV) RNA in saliva and gingival crevicular fluid of HCV-infected patients. J. Clin. Microbiol. 43, 4413–4417.

Takimoto, T., Portner, A., 2004. Molecular mechanism of paramyxovirus budding. Virus Res. 106, 133–145.

Trestard, A., Bacq, Y., Buzelay, L., Dubois, F., Barin, F., Goudeau, A., Roingeard, P., 1998. Ultrastructural and physicochemical characterization of the hepatitis C virus recovered from the serum of an agammaglobulinemic patient. Arch. Virol. 143, 2241–2245.

Wakita, T., Pietschmann, T., Kato, T., Date, T., Miyamoto, M., Zhao, Z., Murthy, K., Habermann, A., Krausslich, H.G., Mizokami, M., Bartenschlager, R., Liang, T.J., 2005. Production of infectious hepatitis C virus in tissue culture from a cloned viral genome. Nat. Med. 11, 791–796.

Yi, M.K., Villanueva, R.A., Thomas, D., Wakita, T., Lemon, S.M., 2006. Production of infectious genotype 1a hepatitis C virus (Hutchinson strain) in cultured human hepatoma cells. Proc. Natl. Acad. Sci. U.S.A. 103, 2310–2315.

Yoshioka, H., Mikami, M., Mori, Y., Tsuchida, E., 1994. A synthetic hydrogel with thermoreversible gelation. J. Macromol. Sci. A31, 113–120.

Zhong, J., Gastaminza, P., Cheng, G., Kapadia, S., Kato, T., Burton, D.R., Wieland, S.F., Uprichard, S.L., Wakita, T., Chisari, F.V., 2005. Robust hepatitis C virus infection in vitro. Proc. Natl. Acad. Sci. U.S.A. 102, 9294–9299.

Available online at www.sciencedirect.com
SCIENCE DIRECT
VIROLOGY
Virology 345 (2006) 434 – 445
www.elsevier.com/locate/yviro

Down-regulation of the internal ribosome entry site (IRES)-mediated translation of the hepatitis C virus: Critical role of binding of the stem-loop IIId domain of IRES and the viral core protein

Takashi Shimoike [a,*], Chika Koyama [a], Kyoko Murakami [b], Ryosuke Suzuki [b], Yoshiharu Matsuura [c], Tatsuo Miyamura [a,b], Tetsuro Suzuki [b,*]

[a] *Department of Virology II, National Institute of Infectious Diseases, Musashi-murayama, Tokyo 208-0011, Japan*
[b] *Department of Virology II, National Institute of Infectious Diseases, Shinjuku-ku, Tokyo 162-8640, Japan*
[c] *Research Center for Emerging Infectious Diseases, Research Institute for Microbial Diseases, Osaka University, Suita-shi, Osaka 565-0871, Japan*

Received 27 May 2005; returned to author for revision 1 July 2005; accepted 7 October 2005
Available online 17 November 2005

Abstract

In a previous study, we observed that hepatitis C virus (HCV) core protein specifically inhibits translation initiated by an HCV internal ribosome entry site (IRES). To investigate the mechanism by which down-regulation of HCV translation occurs, a series of mutations were introduced into the IRES element, as well as the core protein, and their effect on IRES activity examined in this study. We found that expression of the core protein inhibits HCV translation possibly by binding to a stem-loop IIId domain, particularly a GGG triplet within the hairpin loop structure of the domain, within the IRES. Basic-residue clusters located at the N-terminus of the core protein have an inhibitory effect on HCV translation, and at least one of three known clusters is required for inhibition. We propose a model in which competitive binding of the core protein for the IRES and 40S ribosomal subunit regulates HCV translation.

Keywords: Hepatitis C virus; Internal ribosome entry site; Translation; Core protein

Introduction

Hepatitis C virus (HCV) is a major causative agent of chronic hepatitis, liver cirrhosis, and hepatocellular carcinoma (Alter and Seeff, 2000; Pawlotsky, 2004). HCV contains approximately 9.6 kb of positive-strand RNA with one open reading frame encoding a precursor polyprotein, which is proteolytically cleaved to produce the mature structural and non-structural proteins of HCV (Choo et al., 1991; Grakoui et al., 1993; Hijikata et al., 1991; Takamizawa et al., 1991). Although HCV exhibits considerable genetic diversity, the 5′ untranslated region (5′UTR) of the viral genome is relatively well conserved among all genotypes.

HCV translation is initiated by a cap-independent mechanism involving an internal ribosome entry site (IRES), comprising nearly the entire 5′UTR of the genome. There is evidence to suggest that the first 12 to 30 nucleotides (nt) of the coding sequence are also important for IRES activity (Hellen and Pestova, 1999; Lu and Wimmer, 1996; Reynolds et al., 1995). The proposed secondary structure of the HCV 5′UTR, thought to contain four major domains (I to IV) (Fig. 1), may be conserved among HCV and related flaviviruses and pestiviruses (Brown et al., 1992; Honda et al., 1999a, 1999b; Zhao and Wimmer, 2001).

Recruitment of the 43S ribosomal complex, containing a small 40S ribosomal subunit, eukaryotic initiation factor (eIF) 3, and a tRNA–eIF2–GTP ternary complex, to mRNA molecules is critical for initiation of eukaryotic protein synthesis. The 40S subunit and eIF3 can bind independently to the HCV IRES (Buratti et al., 1998; Hellen and Pestova, 1999; Kieft et al., 2001; Sizova et al., 1998). However, it appears that interaction between IRES RNA and the 40S

* Corresponding authors. T. Shimoike is to be contacted at fax: +81 42 561 4729. T. Suzuki, fax: +81 3 5285 1161.
E-mail addresses: shimoike@nih.go.jp (T. Shimoike), tesuzuki@nih.gi.jp (T. Suzuki).

0042-6822/$ - see front matter © 2005 Elsevier Inc. All rights reserved.
doi:10.1016/j.virol.2005.10.013

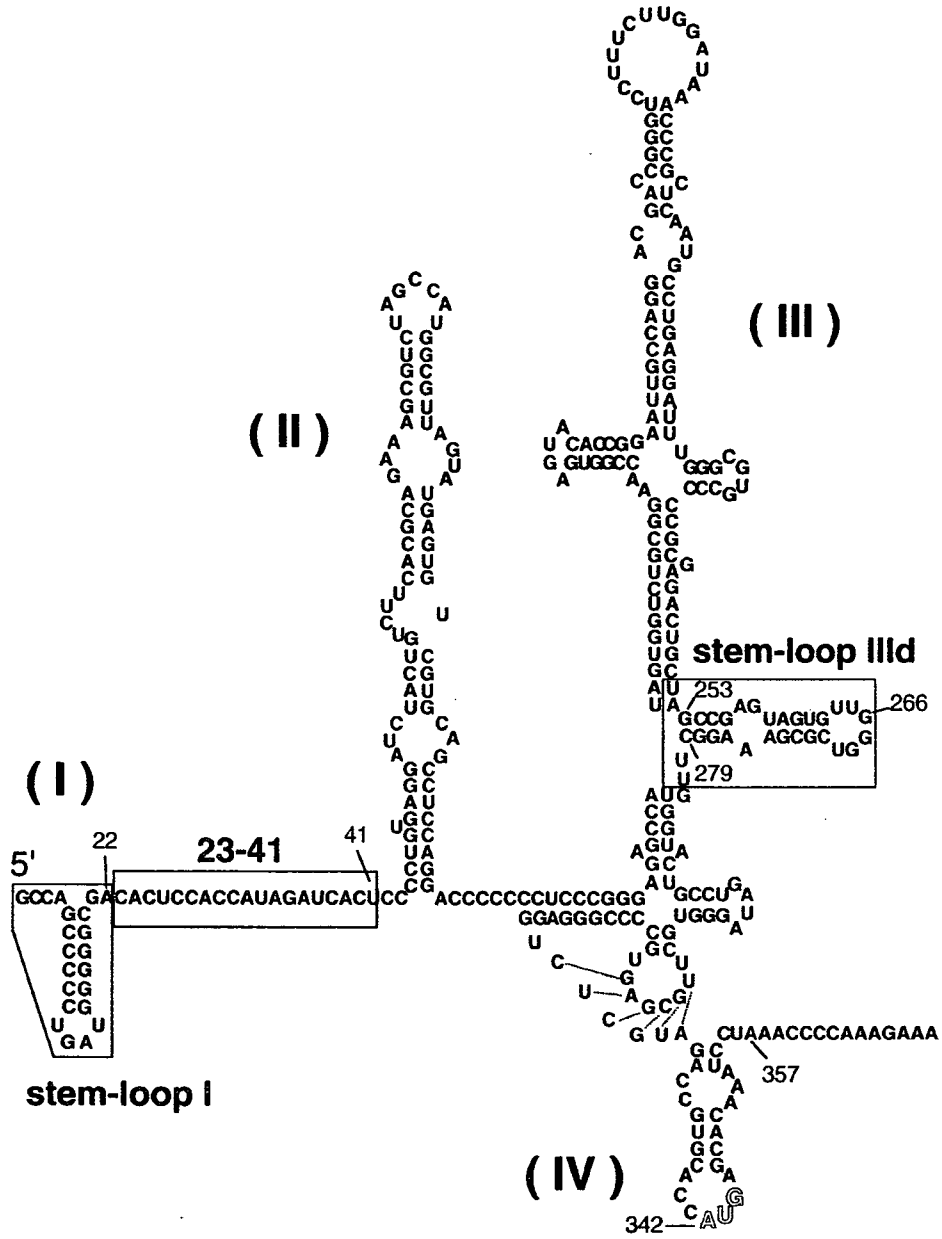

Fig. 1. Predicted secondary structure of the HCV 5′UTR (Honda et al., 1999a, 1999b). The stem-loop I, nt 23–41, and stem-loop IIId domains are highlighted. The initiator AUG codon is shown in the sequence of loop IV. Small numerals indicate the nucleotide positions from the 5′end.

subunit drives formation of the IRES-40S subunit–eIF3 complex since HCV IRES RNA demonstrates similar affinity for the 40S subunit and the 40S–eIF complex (Kieft et al., 2001). Other cellular factors such as La autoantigen (Ali et al., 2000; Ali and Siddiqui, 1997; Isoyama et al., 1999), heterogeneous ribonucleoprotein L (Hahm et al., 1998), poly-C binding protein (Fukushi et al., 2001; Spangberg and Schwartz, 1999), and pyrimidine tract-binding protein (Ali and Siddiqui, 1995; Anwar et al., 2000) also bind to the IRES element and modulate translation.

HCV core protein, which is located at the N-terminus of the viral polyprotein, is a putative nucleocapsid protein given the basic nature of its amino acid (aa) residues and the organization of the HCV genome. HCV core protein can form multimeric complexes, as well as heterodimer complexes with envelope E1 protein (Lo et al., 1996). Physical interaction between the core protein and viral genomic RNA is thought to occur during nucleocapsid formation. The results of several Northwestern analyses suggest that the core protein binds to the 5′UTR of the HCV genome, regardless of the specific RNA sequences involved (Santolini et al., 1994; Hwang et al., 1995; Fan et al., 1999). We previously used both in vivo and in vitro systems to demonstrate that the core protein preferentially binds to positive-stranded viral RNA containing the 5′UTR and